BNL-16705

The Structure of Neutron Resonances*

R. E. Chrien
Brookhaven National Laboratory
Upton, New York 11973

Lectures prepared for
International School on Nuclear Structure
Alushta (Crimea), U.S.S.R.
April 13-28, 1972

*Work supported by the United States Atomic Energy Commission.

ABSTRACT

Certain topics relevant to the structure of neutron resonances are discussed in these lectures. A summary of experimental techniques for resonance studies via the (n,γ) reaction and the inverse (γ,n) reaction is given. Experiments relating to direct reaction mechanisms, partial width correlations, pygmy resonances, and doorway states are described.

I. INTRODUCTION AND MEASURING TECHNIQUES

Shortly after the discovery of the neutron by Chadwick in 1932 [1], it was found that the absorption of these particles by matter was a highly selective process. The fact that neutron absorption occurs in very narrow energy regions formed the early experimental evidence for the existence of long-lived nuclear states and Bohr's theory of the compound nucleus. The sharply-defined metastable states of the compound nucleus exist only at low excitation energies so that only a relatively few reaction channels are open; in contract, at higher energies the capture cross sections exhibit a monotonic behavior with energy. This is the region where $\Gamma \gg D$. For low energies, however, the resonant states are almost stationary, being characterized by mean lives in the range 10^{-13} to 10^{-15} seconds. Very near the excitation corresponding to the neutron separation energy, the radiative decay widths compete favorably with neutron emission, and $\Gamma_\gamma \sim \Gamma_n$ for many resonances.

The fundamental properties of the neutron interaction were discovered in a painstaking series of experiments undertaken, largely at the Cavendish Laboratory, in 1933 and 1934. The use of moderating materials and crude filters established properties such as the very high cross sections for low velocity neutrons and the selective capture process. A great technical revolution occurred shortly after the discovery of fission, as it became clear that a knowledge of the neutron cross section and its resonances would provide vital information in nuclear energy applications. It became important to measure carefully neutron energies and to provide intense sources.

The time-of-flight method has proved to be useful for slow neutrons. With a neutron velocity of only 2200 meters/sec at 0.0253 electron volts, it became feasible for Dunning and his collaborators [2] to develop a mechanical monochromator or velocity selector for slow neutron studies in 1935. Later refinements resulted in the well-known neutron chopper designs exemplified by the Brookhaven design of Seidl [3], which were used in combination with high flux reactors. Monoenergetic neutrons were also available from Bragg reflection, as demonstrated by Zinn [4], since the appropriate slow neutron wavelength, $\lambda = 1.82$ Å at 0.0253 eV is comparable to crystalline lattice spacings. Many of the early, low-energy cross section measurements were made with neutron crystal monochromators.

Although reactors continue to be useful neutron sources, the most versatile pulsed and continuous sources are accelerator-based. These make use of specific reactions such as Li-7 (p,n), or non-specific reactions such as proton-induced evaporation spectra and electron-induced bremsstrahlung photoneutron sources. These non-specific reactions produce continuous or "white" energy spectra, and for most applications offer the best all-around source. Outstanding examples in the U.S. are the Nevis Synchro cyclotron and the contemplated Los Alamos linear proton accelerator, for proton-induced sources; and the Oak Ridge Electron Linear Accelerator, for the photoneutron sources. A table of instantaneous source strengths is given below, and shows the impressive increase in neutron output over the past 30 years.

TABLE I: Source Strengths

Radioactive Sources (PuBe, RaBe)	$\sim 10^6$ n/sec
Reactors	10^{12}-10^{15} n/sec
Accelerators (Linacs or Cyclotrons)	10^{17}-10^{19} n/sec
Nuclear Detonations	$> 10^{24}$ n/sec

Since the area covered in these lectures is to be restricted to the well-defined resonance region, we restrict our attention to the elastic reaction channel and to the various radiative channels, omitting for the moment the subject of neutron induced fission. The simplest possible measurement is that of the total cross section, since only a transmission experiment is required. The condition that the levels be well separated usually holds, and the Breit-Wigner single-level is then valid in the low-energy, $\ell = 0$ region (neglecting potential scattering and 1/v dependence):

$$\sigma(x) = \sigma_o/1+x^2 \qquad x = 2(E-E_o)/\Gamma \qquad \Gamma = \Gamma_n + \Gamma_\gamma$$

$$\text{and } \sigma_o = 4\pi\lambda\!\!\!^{-}{}_o^2 g\ \Gamma_n/\Gamma$$

From only total cross section information, a limited amount of information can be derived about the structure of these quasi-stationary states. From measurements of the peak position, shape, or area, one can obtain the quantities $\lambda\!\!\!^{-}{}_o^2$ (or E_o), $g\Gamma_n/\Gamma$, and Γ. From simple auxiliary experiments on the scattering channel, one can additionally determine Γ_n/Γ. The parameter $\Gamma_\gamma = \Gamma - \Gamma_n$, however contains many radiative exit channels and conceals, therefore, a wealth of information not revealed by total cross section or scattering measurements. In practice it is in fact quite difficult to determine g, separately for many resonances, and the radiative channel information can be used to establish this parameter.

The measurement of the gamma-ray spectrum following resonance neutron capture determines the set of $\Gamma_{\gamma i}$ for the individual resonances, where $\Gamma_\gamma = \Sigma\Gamma_{\gamma i}$, and the individual width may be related to the electromagnetic transition matrix elements. In the electric dipole case, of major concern, for example:

$$\Gamma_{if} = \frac{16\pi k^3}{9} \frac{|< X_i(J_i)||\mathcal{K}_E^{(1)}||X_f) >|^2}{(2J_i + 1)} ;\ i \to f$$

In many cases the structure of the final states f will be known from other experiments; in these instances the radiative widths will provide some insight into the structure of the initial states i.

The history of neutron capture γ-ray spectroscopy is virtually as old as that of the neutron itself. In experiments carried out just after Chadwick's discovery, Fermi and his collaborators [5] established that neutron capture was an important process at low bombarding energies.

By chemical separations, Fermi's group had discovered that several distinct kinds of interactions were responsible for the radioactivity induced by neutron bombardment. Since several of the radioactive products, namely bromine and iodine, were found to be isotopes of the element under bombardment, they concluded that neutron capture, followed by the emission of γ rays, was responsible for the activity in these cases. Meanwhile, at Cambridge, D. E. Lea made the first direct observation of neutron capture γ rays in the course of investigations of neutron scattering from paraffin and liquid hydrogen [6]. In these experiments, Lea noticed that radiation was emitted in the backward direction, at angles between 120° and 180° to the incident beam. Because of the direction of emission he observed, and because of the differences in specific ionization of this radiation in detection chambers filled with argon and hydrogen, Lea concluded that this radiation was composed of γ rays emitted by the capture of neutrons by protons to form deuterium. By interposing lead absorbers, he estimated that the γ-ray energy lay between 2 and 4 MeV.

A measure of the vast technical progress achieved in this field in the intervening 35 years is the fact that the hydrogen capture γ ray is now known to a precision of 20 parts per million, namely its energy is found to be $2223.29 \pm .07$ keV [7]. In part because of the tremendous technical progress achieved since Lea's early work, the study of capture γ-ray spectra has contributed significantly to our understanding of nuclear physics.

Crucial to the success of recent work in neutron resonance spectroscopy is the simultaneous development of high resolution, high efficiency radiation detectors and high intensity neutron sources. Although neutron intensity is not usually a problem in thermal neutron capture, in resonance capture typical beam strengths are extremely low. This is because the combination of a pulsed source and a long flight path effectively result in beam intensities $\sim 10^{5}$ smaller than thermal capture work. Hence resonance capture studies are generally carried out with single Ge(Li) spectrometers. Ge(Li) detectors are now available with resolutions of the order of 0.07% at 7.6 MeV, as is shown in Fig. 1 where is depicted the separation of the 7632, 7645 keV transitions to the 14 keV excited and ground states of Fe-57.

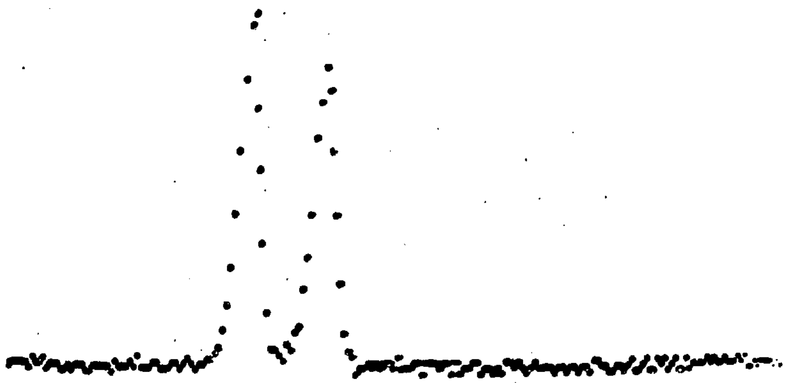

Fig. 1 Ge(Li) detector performance. The 7645.6 and 7631.4 keV transitions in Fe-57. The gain is 0.774 keV/channel.

Let us now examine some of the simple features of the neutron capture reaction. The masses of the final nucleus and the sum of the target nucleus and neutron mass differ by about 8 MeV for the heavy elements. This difference, added to the kinetic energy of the incoming neutron, goes into the nuclear excitation. For low neutron energies, γ-ray emission is highly probable, and the difference in excitation energies goes into the γ-ray energy, except for a small amount which is carried away by the recoiling nucleus. In Fig. 2, a schematic level scheme is shown. We can see that near 8 MeV the levels are densely spaced, of the order of a few eV for many nuclei. These levels are particle unbound, being above the neutron separation energy, but they are well-defined and long lived. They are extremely complex states in general. Near the ground state the states are widely spaced and consist of simple nucleon motions, either singly, in well-defined shell model orbits, or collectively in coherent motions such as vibrations or rotations. The γ-ray transition thus connects these two remarkably different kinds of states.

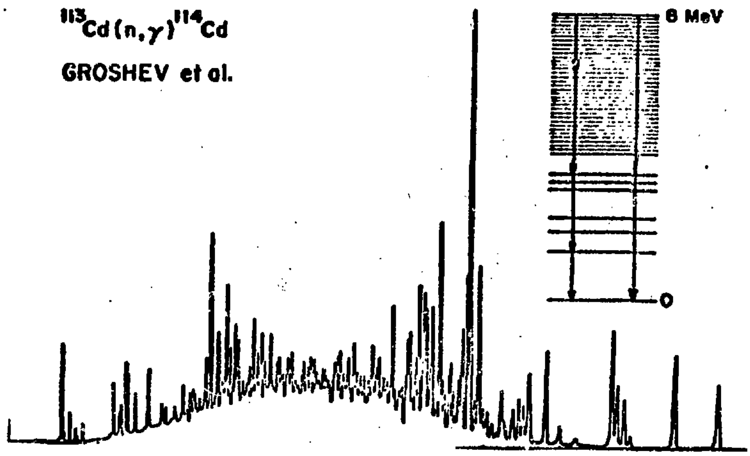

Fig. 2 A typical capture γ-ray spectrum, as recorded by a magnetic pair spectrometer.

Figure 2 also shows a complete capture spectrum taken with the magnetic Compton spectrometer of Groshev, for cadmium [8]. At the high energy end, the discrete, well-separated transitions from the resonant states to the low-lying states are seen. At the low energy end one sees γ rays which represent transitions between the low-lying states. The middle of the spectrum is extremely complex, representing a mixture of cascade γ rays and transitions to states of high excitation. Most of our interest will be focused on either the high energy or low energy ends of these spectra, the middle portion being much more difficult to interpret.

Capture γ-ray experiments may be classified into three types, depending on the energy selection of the incoming neutron. In thermal capture, the neutrons are obtained from a Maxwellian distribution with a temperature such that most of the neutrons have energies close to 0.025 eV. Nuclear reactors are copious sources of such neutrons. Very little can be learned about the capturing states in these experiments, since there is no way to vary the neutron energy. They are principally useful in providing information on the final states of the residual nucleus. In the so-called average capture experiments, the sample is exposed to a broad range of neutron energies, from a few electron volts up to several MeV. In this experiment, only average properties of the capturing states can be determined. Spins and parities for final states, however, can be deduced. The most detailed information is obtained, in principle by measuring spectra of γ rays emitted as a function of incoming neutron energy. By using time-of-flight techniques to separate the capturing states, information is obtained, both for the highly excited states near the neutron separation energy and for the low lying nuclear levels. Such a technique is used at the BNL High Flux Reactor experiments, where a neutron chopper is used to produce a pulsed neutron beam [9].

The chopper uses beam hole H-2 at the HFBR, which is a 40 MW heavy water-moderated and cooled research reactor. As can be seen from Fig. 3, H-2 beam is a radial one and contains a relatively large proportion of high energy neutrons. Table II lists the parameters of this beam and also lists the relevant parameters of the chopper, which is driven routinely at a speed of 15000 RPM by a 3-phase alternating current source from a 5 KW electronic generator.

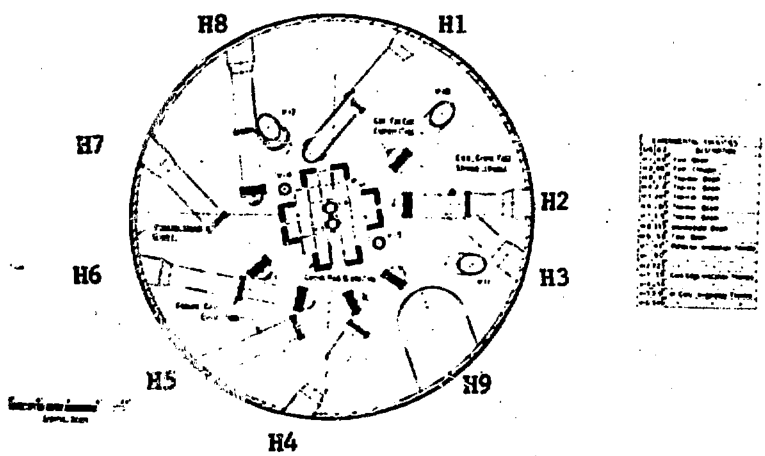

Fig. 3 Plan view of HFBR beam tubes. H-2 is used by the chopper for time of flight studies.

TABLE II

H-2 Beam and Chopper Parameters

At thimble tip	Φ_{th}	$\cong 7\times10^{14}$ n/sec/cm^2
	Φ_{epi}	$= 2.9\times10^{13}$ n/sec/cm^2 $\log_e$ energy interval
	$\Phi_{fission}$	$= 4.6\times10^{13}$ n/sec/cm^2

Chopped beam flux at 22 meters	8×10^3 n/sec/cm^2/$\log_e$ energy interval
Burst widths	5.0 μsec at 15000 RPM
Repetition rate	1000/sec

Power required at 15K in 15μ vacuum $\cong$ 1400 watts

An inpile collimator 1 meter in length and containing a grid of openings 2.5x2.5 mm provides a rather severe vertical and horizontal collimation.

The slit system is formed of nickel plates held between quadrants of sintered tungsten. The rapidly rotating slit system is contained within forgings of high strength "maraging" steel, as shown in Fig. 4. The pulsed neutron beam formed by the chopper is allowed to travel down a

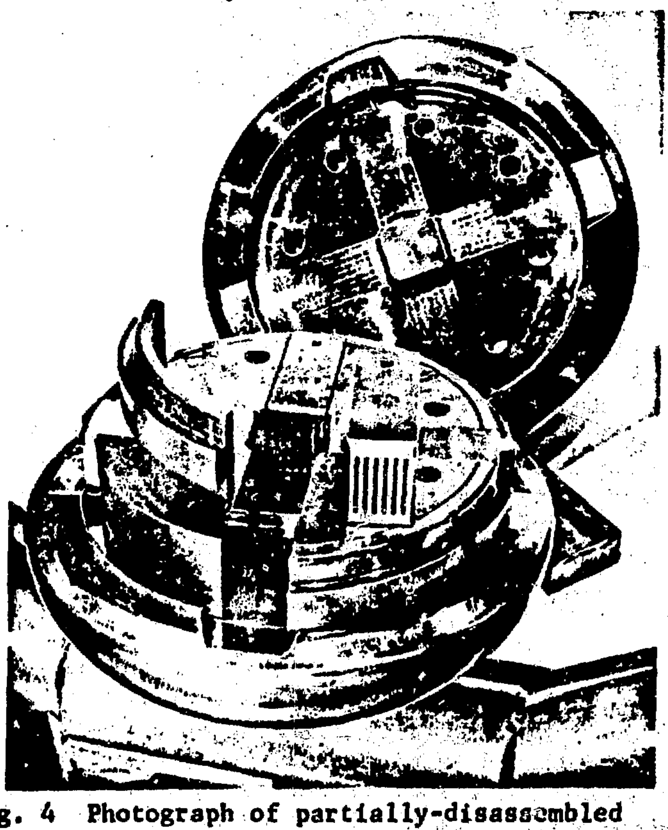

Fig. 4 Photograph of partially-disassembled fast chopper rotor.

48-meter long flight path, through an evacuated tube emerging from the reactor, as depicted in the next Fig. 5. There is an intermediate station at 22 meters within the reactor building. The detector station, in which a temperature-controlled environment is maintained, is located on a pedestal some twenty feet above ground level. The time information

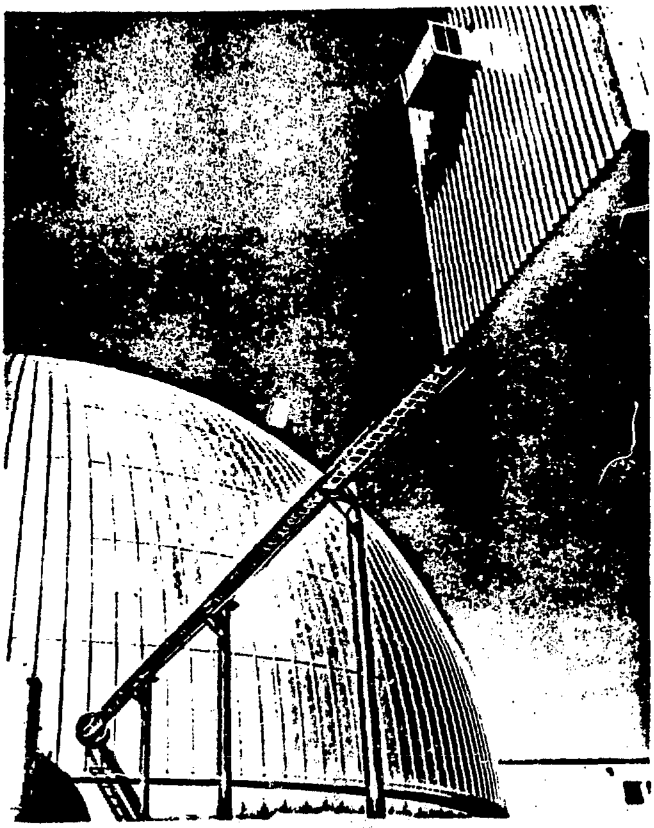

Fig. 5 The 48-meter HFBR fast chopper flight station.

determines the energy of the captured neutron and from this and the neutron separation energy, one may determine the excitation energy of the compound nucleus. The two parameters, time and pulse height, are decoded into 10 bit and 11 bit binary numbers respectively, and written on magnetic tape for each γ-ray event. Such a multiparameter experiment requires a sophisticated data processing system, based on using an XDS-910 computer with a 16192 24 bit-word memory. Two independent analog-digital converters are interfaced to the computer, allowing another single-parameter experiment. Thus in principle thermal and resonance capture experiments can be run simultaneously.

The amplifying system consisting of a charge sensitive preamplifier followed by a main amplifier employing active filtering techniques for noise minimization. The digitizer contains an automatic gain stabilizing circuit using a stabilized precision pulser as a reference source. We will discuss a little later some of the specific problems arising from the high instantaneous data rates which can be present in a time of flight experiment.

To clarify further the two-parameter nature of these experiments one may refer to Fig. 6, which is a pictorialization of the way the data are organized. In this figure the top axis represents the neutron capture cross section. A cut along this axis at a particular neutron energy may be taken for the purpose of obtaining a γ-ray spectrum. We are in a position, then, to obtain a spectrum at thermal energies, or in the resonance region, whether it be on resonance or in between resonances. In this fashion, the detailed behavior of each transition can be followed as a function of neutron energy.

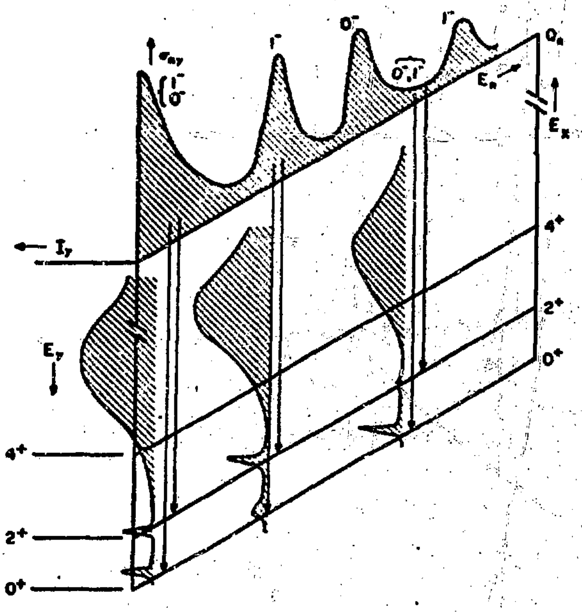

Fig. 6 Structure of a 2 parameter--time-of-flight and γ-ray pulse height--experiment on neutron capture.

Each magnetic tape reel, 2400 feet long, contains approximately 3.3×10^6 events and these tapes are scanned later at the laboratory's CDC-6600 computer. Since individual events are recorded, a variety of possible spectra are obtained--for example, a time-of-flight spectrum for an individual γ-ray transition, or a pulse height spectrum for a given time of flight region. Least squares fitting of peaks is then carried out in a conventional manner.

Figure 7 shows typical γ-ray spectra, that for the 46 and 41 eV resonances in Yb-171. We shall discuss in due course some of the implications of these spectra for the capture reaction mechanism; however, several immediate applications are evident: from the examination of many hundreds of such spectra, a systematic set of measurements of multipole transition strengths in the region of 6-8 MeV are obtained.

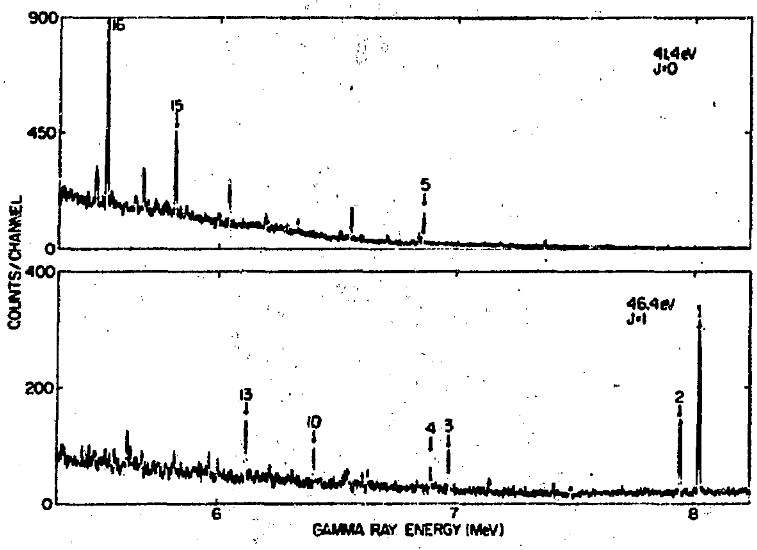

Fig. 7 A typical resonance capture spectrum from Yb-171

For most nuclides, only dipole transitions are important, hence as is evident from the figure, spin assignments for the resonance states can be obtained. Furthermore it has been shown that the population of final states through multi-step cascades is dependent on initial state spin. The capture spectrum at low energies--50 keV-500 keV will reveal systematic features characteristic of resonance spin. A detailed discussion of all possible types of experiments that can be done with time-of-flight capture spectra is not feasible here, but the following list of experiments done with the BNL facility for the past six years will give some idea of the possibilities. Some of these will be discussed in detail in subsequent sections:

1) Measurements of individual partial radiative widths and their statistical properties, correlations and distributions.

2) Determination of the photon strength functions in the 6-8 MeV region.

3) Resonance spin determinations from high and low-energy capture spectra.

4) Directional correlation experiments with unpolarized beams and $\ell = 1$ resonances. These may be used for initial and final state spin assignments and initial state parity assignments. Recently directional correlations have been applied to obtaining the relative channel spin components in p-wave resonances.

5) Comparison of off-resonance radiative intensities to resonance intensities. The energy dependence of radiative width amplitudes and determination of a direct reaction component.

6) Measurement of isomeric life times through their effect on the time-of-flight dependence of low-energy γ-rays.

7) Isotopic analysis by means of neutron capture γ-rays.

8) Nuclear structure information by virtue of populating low-lying states of the residual nucleus and assigning their spins and parities.

9) Applying capture γ-ray spectral techniques to fissile targets like U-235, Pu-239 for spin determinations of resonances and investigation of the character of the fission γ-ray spectrum.

Other facilities in the U.S. which have been active in capture γ-ray studies include electron linac accelerators at Oak Ridge, Lawrence Laboratory, Livermore, Naval Research Laboratory, and Rensselaer Polytechnic Institute. As employed in neutron capture γ-ray measurements, the ORELA has been able to deliver some 40 kW of power on a water-cooled tantalum target, at an electron energy of 140 Mev. The 40 ns burst employed in conjunction with a 10 meter flight path, and an 800 sec^{-1} repetition rate allows reasonable spectra to be accumulated to several tens of kilovolts for light to medium-A nuclei, and up to $\sim$ 1 keV for heavy nuclei. The neutron current produced at the 10 meter target station is about 42.8 $n/cm^2/sec/eV$ at 1 keV, and the flux distribution with energy is somewhat harder ($\sim E^{-0.8}$) than that produced by a reactor. In the low eV range the beam current available from the accelerator is a factor of 2 to 4 lower than the chopper; however, at higher energies the far superior resolution (by a factor of 125) and harder spectrum allows the accelerators to explore a much higher neutron energy region.

A rather different approach to data recording exists in the ORELA facility, which possesses two computers (SEL 810B) each with a disk memory store. The two-parameter data are stored directly on the fixed head, rapid access disks of 400,000 and 800,000 words [12]. Each one of several experimenters is assigned a portion of the disk for his experiment. The data sorting takes place prior to storage on disk, hence there is no need for later, off line, data organization into spectra. Since all data are not recorded because of disk size limitations, the experimenters must be able to predict in advance which spectra will be useful.

Another important contribution to resonance capture spectra has been made by groups at BNL and Idaho using neutron monochromators. The monochromator developed by Walter Kane at BNL is shown in Fig. 8. A convergent collimator produces a 2.54 cm diameter beam at the crystal position with an intensity of 2×10^9 n/cm^2/sec. The diffracted beam current at the target position is 2×10^5 n/sec at 1 eV, and a useful energy range is 0.01 to 20 eV. A direct beam is obtainable through a 38 cm quartz filter with an intensity

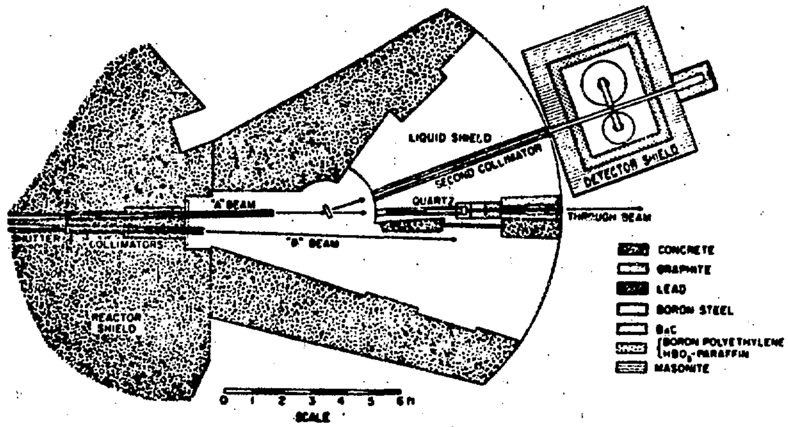

Fig. 8 The BNL resonance capture γ-ray monochromator.

of $\sim 10^8$ n/cm^2/sec and a Cd ratio of 2×10^4. This facility complements a time-of-flight experiment by providing a continuous beam at a single energy instead of a pulsed beam with a continuous energy distribution. For examining a fissile target, for example, it is advantageous to select the neutron energy on target in order to minimize background effects. This device has been particularly successful in establishing a decay scheme for U-236 [10].

Although strictly-speaking not a resonance method, mention should be made of the so-called "average-resonance" technique exploited by Bollinger at Argonne [11]. Figure 9 shows the experimental arrangement. In this technique, the sample is surrounded by boron-10 and placed in the high-flux region of a nuclear reactor. The combination of the 1/v absorber and the 1/E reactor spectrum effectively limits the incident neutron

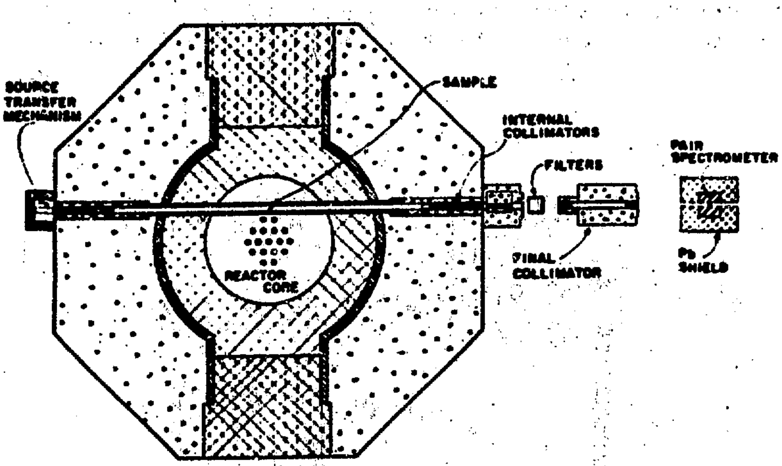

Fig. 9 The ANL in-pile average spectrum facility.

spectrum on the sample to a broad region peaked below 1 keV. A beam of capture γ-rays is taken out of the reactor, filtered to remove neutrons and viewed by an annihilation-pair spectrometer. Because of the high reaction rate in such an arrangement, and the superior solid angle available, the event rates in the average capture experiment exceed that of an external neutron beam experiment by at least one order of magnitude. The broad energy range produces an averaging over a number of resonances which ranges typically from 20 for a medium weight nucleus to $\sim$ 200 for a rare earth nucleus.

A related set of experiments have been performed by Reich, Greenwood, and their collaborators at the MTR reactor in Idaho. In this case a transmission filter allows an approximately monochromatic beam of neutrons out of the reactor [13,14]. The filter relies on the presence of the cross section minimum below a resonance due to the interference between resonance and direct scattering amplitudes. For scandium the interference "window" is near 2 keV; for iron-56, the window is near 25 keV. The filters are typically 1 meter long. The scandium has a FWHM of 700 eV and provides a flux of 5 x 10^6 neut/cm^2/sec in a 1.9 cm diameter; the iron filter has a FWHM of about 4 keV and provides a flux of 2 x 10^5 neut/cm^2/sec. To remove the effects of secondary windows at higher neutron energies Aℓ and S components are added to the filters. There are certain advantages to this arrangement which compensate for the lower reaction rate: the energy spectrum is better defined and lies at higher mean energies. In principle a better average is obtained and by using different filters the average may be studied as a function of neutron energy.

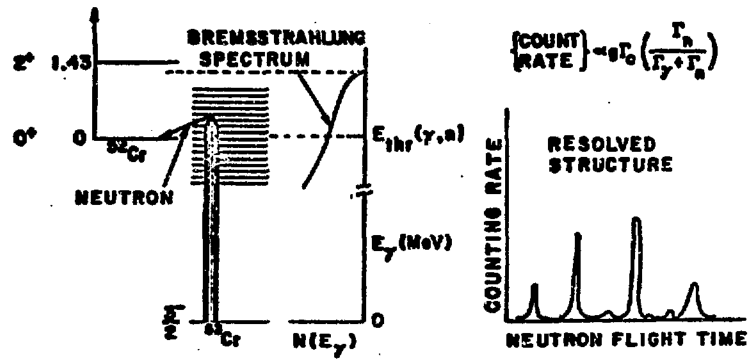

Fig. 10 The structure of threshold photoneutron experiments.

Our discussion of resonance spectroscopy would be incomplete if mention were not made of the photothreshold neutron experiments of Bowman and collaborators at Livermore and of Jackson at the Argonne National Laboratory. The idea of the threshold photoneutron technique is illustrated in Fig. 10. A bremsstrahlung beam of precisely determined maximum energy is employed to excite the target nucleus at just above the neutron separation energy. Only a small number of states is thereby excited and these states decay by neutron emission to the ground state of the residual nucleus or by radiative decay to lower states of the target. The resonance yield is given by integrating the Breit-Wigner cross section:

$$A(\gamma) = 2\pi^2 ƛ^2 g \Gamma_{\gamma o} \Gamma_n / \Gamma$$

The resulting neutron spectrum can be observed with time-of-flight techniques. For all practical cases $\Gamma_n/\Gamma \approx 1$ and the yield is therefore proportional to the ground state radiation width $\Gamma_{\gamma o}$. The angular distributions can also be measured to identify resonance spins and parities.

As an example of the apparatus used to implement this technique, Fig. 11 shows the Argonne facility. The accelerator is a 2-section L-band electron linear accelerator operating from 4-22 MeV with a pulse width of 6 ns and a repetition rate of 720 sec^{-1}. The peak current is between 10 and 20 amperes and is magnetically analyzed to achieve an energy spread of less than 300 keV. A 20 mil silver foil is used as the bremsstrahlung converter; silver having a desirably high neutron threshold.

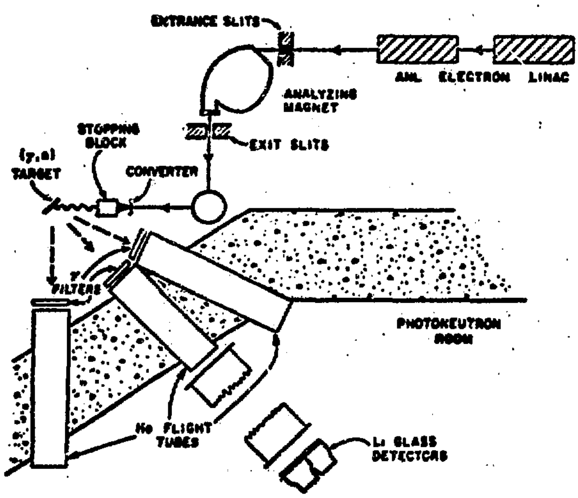

Fig. 11 The ANL photoneutron facility.

These experiments have been directed toward measurement of the electric and magnetic dipole radiation strengths of a variety of nuclei, as well as the distribution of strength with excitation energy. The presence of direct reaction components and intermediate structure has also been reported.

In the balance of these lectures we shall examine the applications of these techniques to several topics of current interest. These topics have to do with the failure of the compound nuclear states to achieve the complexity usually associated with these high excitation energies. These topics deal, then, with the non-statistical behavior of the resonance decay patterns. Several valuable reviews are available which present summaries of the experimental techniques [15-18]. The recent Statistical Properties of Nuclei Conference, at Albany is an important reference for much of the latest work [19]. Let me stress that this review is by no means complete. My sources for these discussions will mainly be experiments carried out with the facilities I have described in the United States. A familiarity is assumed here with the important contributions to resonance spectroscopy carried out in the USSR and Western Europe, and these will be discussed only in a peripheral manner.

Similarly, most of the discussion will center on the radiative channels, and no attempt will be made to summarize, for example, the effect of the fission barrier on resonances, nor any discussion of the statistics of neutron widths and level spacings. For reviews of these topics, the reader is referred to reference 19.

II. THE DIRECT CAPTURE MECHANISM

The formal theory of Wigner and Eisenbud on particle reactions was modified by Lane and Thomas in 1958 to include photons [20]. They showed that not only does the radiative width include contributions from closed and open channels in the external region, $r > R$; but also that the capture amplitude includes a non-resonant part, analogous to the potential scattering amplitude which must be added to elastic scattering. This direct amplitude, for E-1 radiation may be written [21]:

$$A(E1) = \left(\frac{16\pi}{9}\frac{k^3}{\hbar}\right)^{\frac{1}{2}}\left[\frac{i\bar{e}\pi^{\frac{1}{2}}}{k_c}\int_{ext} dr_\alpha \{I_\ell(r_\alpha) - e^{-i\phi\ell} O_\ell(r_\alpha)\} r_\alpha^2 u_f(r_\alpha)\right] \times \frac{J||Y^{(1)}||J_f}{(2J+1)^{\frac{1}{2}}}$$

where the symbols have their usual meaning and u_f, the final state radial wave function is proportional to the reduced width amplitude of the final state. The above expression is not quite complete, for it contains only the external portion of the region of integration. The major portion of the potential capture--that is the non-resonant portion of the amplitude--is expected to be described by this expression; the remainder being due to the effect of far away levels. This major component is termed the "hard sphere matrix element."

Lane and Lynn gave an expression for the hard sphere capture, for s-wave neutrons at low energies [22]:

$$\sigma\ (\text{hard sphere}) = \frac{0.062}{R\sqrt{E_n}}\left(\frac{Z}{A}\right)^2 \theta_f^{\,2}\, y^2 \left(\frac{y+3}{y+1}\right)^2 \text{ barns}$$

$$A(\gamma) = 2\pi^2 \lambda\!\!\!^{-}{}^2 g \Gamma_{\gamma o} \Gamma_n / \Gamma$$

The resulting neutron spectrum can be observed with time-of-flight techniques. For all practical cases $\Gamma_n/\Gamma \approx 1$ and the yield is therefore proportional to the ground state radiation width $\Gamma_{\gamma o}$. The angular distributions can also be measured to identify resonance spins and parities.

As an example of the apparatus used to implement this technique, Fig. 11 shows the Argonne facility. The accelerator is a 2-section L-band electron linear accelerator operating from 4-22 MeV with a pulse width of 6 ns and a repetition rate of 720 sec^{-1}. The peak current is between 10 and 20 amperes and is magnetically analyzed to achieve an energy spread of less than 300 keV. A 20 mil silver foil is used as the bremsstrahlung converter; silver having a desirably high neutron threshold.

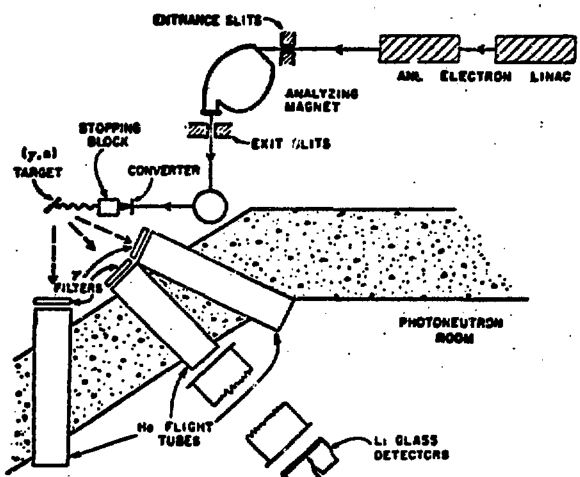

Fig. 11 The ANL photoneutron facility.

These experiments have been directed toward measurement of the electric and magnetic dipole radiation strengths of a variety of nuclei, as well as the distribution of strength with excitation energy. The presence of direct reaction components and intermediate structure has also been reported.

In the balance of these lectures we shall examine the applications of these techniques to several topics of current interest. These topics have to do with the failure of the compound nuclear states to achieve the complexity usually associated with these high excitation energies. These topics deal, then, with the non-statistical behavior of the resonance decay patterns. Several valuable reviews are available which present summaries of the experimental techniques [15-18]. The recent Statistical Properties of Nuclei Conference, at Albany is an important reference for much of the latest work [19]. Let me stress that this review is by no means complete. My sources for these discussions will mainly be experiments carried out with the facilities I have described in the United States. A familiarity is assumed here with the important contributions to resonance spectroscopy carried out in the USSR and Western Europe, and these will be discussed only in a peripheral manner.

Similarly, most of the discussion will center on the radiative channels, and no attempt will be made to summarize, for example, the effect of the fission barrier on resonances, nor any discussion of the statistics of neutron widths and level spacings. For reviews of these topics, the reader is referred to reference 19.

II. THE DIRECT CAPTURE MECHANISM

The formal theory of Wigner and Eisenbud on particle reactions was modified by Lane and Thomas in 1958 to include photons [20]. They showed that not only does the radiative width include contributions from closed and open channels in the external region, $r > R$; but also that the capture amplitude includes a non-resonant part, analogous to the potential scattering amplitude which must be added to elastic scattering. This direct amplitude, for E-1 radiation may be written [21]:

$$A(E1)=\left(\frac{16\pi}{9}\frac{k^3}{\hbar}\right)^{\frac{1}{2}}\left[\frac{i\bar{e}\pi^{\frac{1}{2}}}{k_c}\int_{ext} dr_\alpha\{I_\ell(r_\alpha)-e^{-i\phi\ell}O_\ell(r_\alpha)\}r_\alpha^2 u_f(r_\alpha)\right]x\frac{J||Y^{(1)}||J_f}{(2J+1)^{\frac{1}{2}}}$$

where the symbols have their usual meaning and u_f, the final state radial wave function is proportional to the reduced width amplitude of the final state. The above expression is not quite complete, for it contains only the external portion of the region of integration. The major portion of the potential capture--that is the non-resonant portion of the amplitude--is expected to be described by this expression; the remainder being due to the effect of far away levels. This major component is termed the "hard sphere matrix element."

Lane and Lynn gave an expression for the hard sphere capture, for s-wave neutrons at low energies [22]:

$$\sigma \text{ (hard sphere)} = \frac{0.062}{R\sqrt{E_n}}\left(\frac{Z}{A}\right)^2 \theta_f^2\, y^2 \left(\frac{y+3}{y+1}\right)^2 \text{ barns}$$

where θ_f^2 is the dimensionless reduced width $\gamma^2/\hbar^2/MR^2$, of the final $\ell = 1$ bound state and $y = kR$, k being the wave number corresponding to the radiation to state f, R in 10^{-13} sec, E_n the incident neutron energy, in eV. One of the significant points in this formula is the appearance of the θ^2 term. Groshev, in 1958, pointed out that for many nuclei with A < 70, there is a demonstrable correlation between (n,γ) strengths in thermal capture, and the corresponding (d,p) cross sections to the same states [23].

The direct capture cross section has been computed by Lynn for the intermediate coupling case, using Woods-Saxon potential [21]. The result for V_o = -42 MeV, W_o = 3.36 MeV, V_o = 1.35f and d = 0.58f is shown in Fig. 12. The calculation shows an interesting structure near the 3s giant resonance, where the double peak in the direct cross section is associated with the maximum and minimum in the potential scattering cross section. The calculation shows that the peak value of the direct cross section can be as high as 1 barn or so.

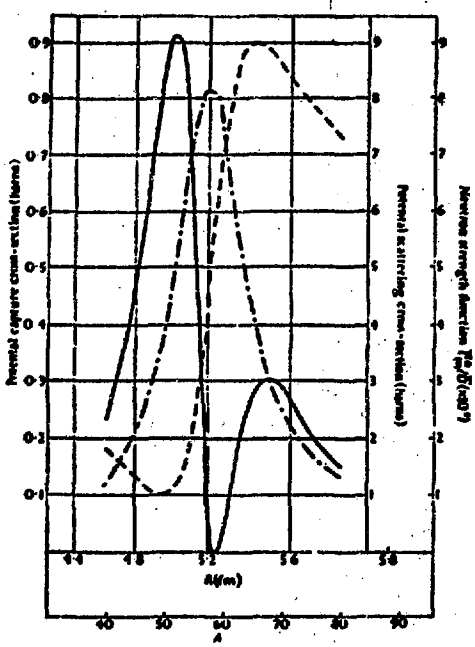

Fig. 12 Non-resonant capture (———), neutron strength function (—·—), and potential scattering (-----) near the 3s giant resonance.

Although the observation of strong high energy transitions to final states with strong single particle character is often cited as evidence for direct capture, a single-energy point measurement does not convincingly establish the non-resonant character of the presumed direct amplitude.

One of the first tasks undertaken by the BNL chopper group was the search for a direct amplitude. Since the amplitude is in itself small, varying as v^{-1}, the search was undertaken by looking for the interference between direct and resonant amplitudes in the vicinity of a resonance.

For the case when levels are well separated we may use the following expression for the capture cross section:

$$\sigma_{n\gamma f} = \pi\lambda\lambda_o \left| D_p^o + \sum_\lambda (\Gamma_{\lambda n}^o)^{\frac{1}{2}} (\Gamma_{\lambda\gamma f})^{\frac{1}{2}} / (E_\lambda - E + i\Gamma_\lambda/2) \right|^2$$

The size of the direct amplitude is measured by the size of D_p^o, where the symbol "o" indicates evaluation at 1 eV.

Striking evidence was found for the presence of D_p^o terms in the case of U-238 [24] and Co-59 [25]. Let us consider this evidence in some detail. In U-238, a spin ½+ target, it has been known since the work of Sheline et al. [26], that at thermal capture, the 4.059 MeV γ-ray, which feeds the ½ member of the ½⁻ [761] orbital at 742 keV in U-239, is much stronger than any other transition, by a factor of ~ 10. Chopper measurements, on the other hand showed this transition to be of quite normal size in resonances, and in particular in the 6.7 eV resonance. A detailed study of the variation in intensity of this transition was undertaken from about 10 eV to thermal. The results are shown in Figs. 13 and 14. Figure 3 shows how the relative intensities of the 4059 and 4068 lines vary across the 6.7 eV resonance, while Fig. 14 shows the relative intensities of the 2 strongest transitions. If as, is commonly done

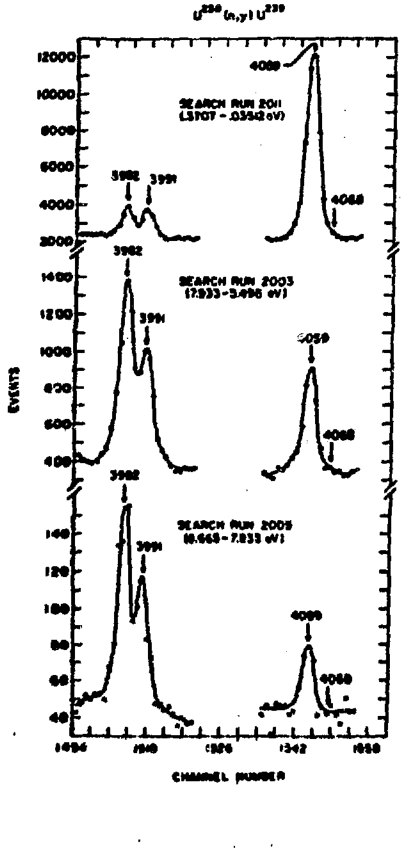

Fig. 13 U-238(n,γ) spectra across the 6.7 eV resonance.

in resonance capture, that the total detector counting rate above some arbitrary low energy limit is proportional to the reaction rate, we can write:

$$\sigma_{\gamma nf}/\sigma_{\gamma}(\text{tot}) = A_i/\Sigma n_i$$

where A_i represents the counts in a single γ-ray peak and $\sum_i n_i$ represents the total counts above the low energy limit. With that assumption we have the results of Fig. 14. Both the 3.982 γ-ray and the 4.059 γ-ray show departures from the usual Breit-Wigner resonance cross section energy dependence. For the 3.982 MeV γ-ray this departure is easily fitted by including interfering amplitudes from higher energy resonances; for the 4.059 MeV γ-ray it is not possible to obtain a fit without the inclusion of at least a term of the size 5×10^{-5} for Dp, or corresponding to $\sigma_{direct}(1\ \text{eV}) \geq 1.6$ mb. This is well within the range of expectation from Lane and Lynn's formula. Supporting evidence comes from (d,p) data; the 820 keV state populated by the 3.982 MeV γ-ray does not exhibit an appreciable (d,p) cross section. The 742 keV state is, however, strongly excited in (d,p).

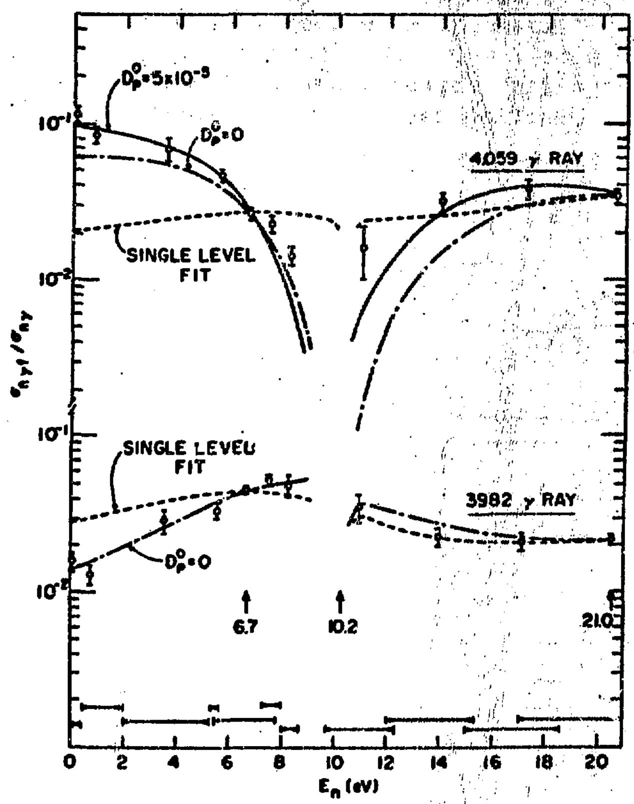

Fig. 14 Interference analysis for two transitions for U-238(n,γ).

One objection to this type of experiment involves the possible influence of bound levels near the neutron separation energy. A bound level with an unusually strong partial width might indeed simulate a direct amplitude. This is unlikely but not impossible for U-238; the known positive levels account for about 2.4 barns out of the 2.73 barns measured at thermal capture. Hence we do not expect a nearby bound level.

A less striking effect has been observed in Co-59, but here it is easier to discount the influence of bound states. Co-59 has a spin of 5/2, and the first resonance at 132 eV has spin 4^-. The level spacing of cobalt is such that we do not expect another 4^- level near thermal. From polarized neutron transmission experiments of Schermer, we know that 78% of the capture is in the 4^- state, the balance being attributable to a bound 3^- level at $\sim$ -80 eV. Figure 15 shows the ratio $\sigma_{\gamma f}/\sigma_{tot}$ for 3 transitions in Co-60. Note that if direct capture is absent, the ground state transition ratio ($4^- \rightarrow 5^+$, 7492 keV) would be relatively weaker at thermal due to the additional 3^- capture admixture in the σ_{tot}. Experimentally, however, we see that the transition is slightly enhanced at thermal, and the curve with the best fit is obtained for a $\sigma(D^o)$ = 9.2 mb. For the 7056 $4^- \rightarrow 5^+$ transition we need no direct term, but the 436 keV level is known to have ℓ = 3 from d,p work. The 7205 $4^- \rightarrow 3^+$ is well fit assuming 5.6 mb of direct capture, but a definite attribution of the amplitude to the direct reaction cannot be made because we may have a significant

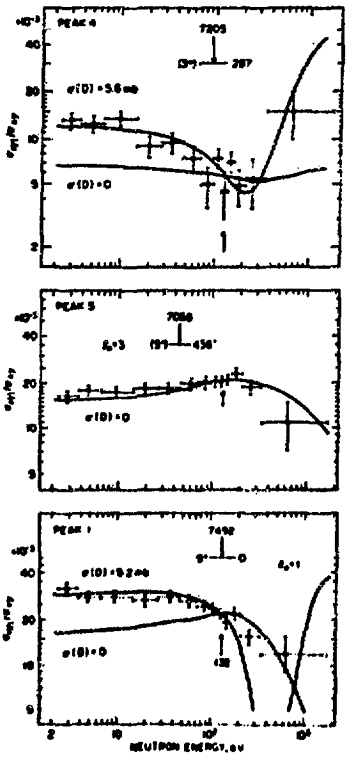

Fig. 15 Interference analysis for three transitions for Co-59(n,γ).

contribution from the 3^- bound level in the case. Interference analyses were carried out for ~ 20 transitions in cobalt; in no case was there discovered any evidence for bound states other than the -80 eV 3^- level. The result for cobalt is in good agreement with theoretical estimates, since the ground state has a reduced width of ½ of the single particle limit.

These results for cobalt were essentially confirmed in unpublished measurement of Auchampaugh [27], although with a somewhat smaller value for σ(direct), 5.5 mb. However, more recently γ-ray circular polarization measurements have been reported in the literature which purport to show that for several transitions, namely those leading to the 3^+ states at 505 and 785 keV, virtually no 4^- capture state is present [28]. The authors interpret their result as indicating a strong destructive interference with a nearby 4^- bound state which had heretofore escaped detection. Assigning capture width amplitudes to this state they can easily explain the partial cross section variation from 0 to 132 eV. To do so, however, they must assume amplitudes which are unreasonably large--the strengths of the 505 and 785 keV lines alone account for 117% of the total radiation width of the hypothesized level, while the same transitions account for 12.4% in the 132 eV resonance.

The interpretation of the data of this circular polarization experiment has in fact been demonstrated to be in error. J. Honzatko and J. Kajfosz [29] have pointed out that in such experiments 3^- and 4^- resonances must be allowed to interfere coherently. This fact has heretofore been overlooked. We may feel confident that the evidence for the supposed bound state is nonexistent.

The third measurement of a direct reaction component comes from the inverse reaction. Bowman and his collaborators have measured the (γ,n) reaction on Pb-208 by the threshold photoneutron technique [30]. A pronounced asymmetry observable at the 1^- 41 keV resonance, Fig. 16, has been interpreted as due to interference with a direct component. The size of the amplitude is surprisingly large, leading to a direct capture cross section of ~ 6 barns at thermal. This is larger than would be inferred from the measured thermal cross section of Pb-207, 0.709 barns. This experiment constitutes a disturbing puzzle. Although Bowman's result has apparently been verified by groups at Argonne and Toronto, a search for the same effect in the (n,γ) reaction, carried out at ORELA by Allen and Macklin, has proved negative. The latter authors estimate that from the observed lack of asymmetry in this reaction, the direct component cannot be larger than 2 mb at 41 keV. Allen and Macklin's results are in accord with the hard sphere capture estimate. The discrepancy suggests the possibility that systematic errors may have to be evaluated carefully for the threshold photoneutron experiments.

An example of how a rather subtle instrumental effects can distort the energy variation of a reaction amplitude was demonstrated several years ago by Frantisek Becvar at Brookhaven. Becvar pointed out that while the average counting rates in a time-of-flight experiment are low, the instantaneous rate on a resonance may be intolerably high. Under high rate conditions, events belonging in the 2-escape peak of a Ge(Li) detector may be displaced by pulse pile up and thrown into the continuum. Accordingly the comparisons of photon intensities on and off resonances may be in error, because the high instantaneous count rate on resonance causes a less than appropriate peak area there. This effect can be rather large. Figure 17 shows a test of the effect in the case of Dy-162(n,γ), in the region of a resonance near 5 eV.

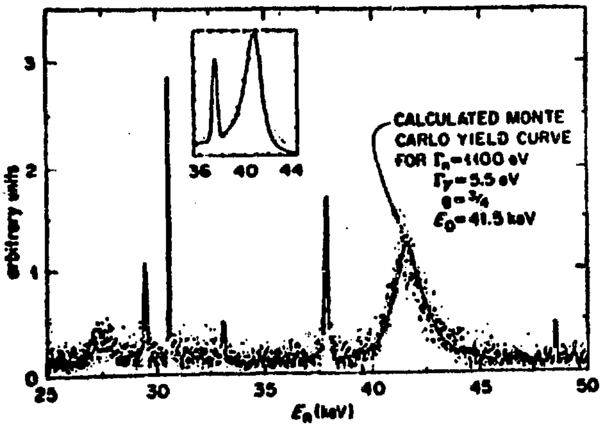

Fig. 16 The 41 keV resonance in Pb-207 as seen in the (n,γ) and (γ,n) reactions.

The time-of-flight response from the Ge(Li) detector, integrated over the entire γ-ray scale above 2.5 MeV is compared to the peak area from a free-running pulser injected into the system. The diminution of pulser counts across the region of the peak is appreciable--25%! The effect can be diminished using appropriately small time constants. A way of doing this, while retaining good resolution and low noise has been developed by Veljko Radeka of BNL [32], and involves a trapezoidal filtering technique.

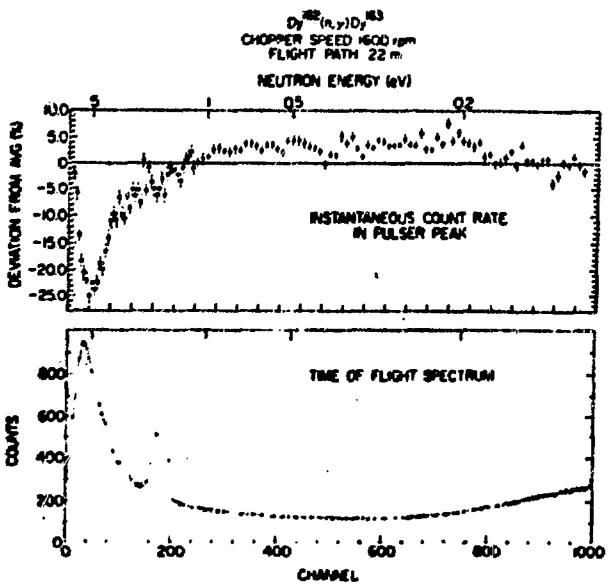

Fig. 17 Counting rate losses in Dy-162 near the 5.45 eV resonance.

After the discovery of this effect, the BNL group reexamined some of the direct capture experiments to see whether a sizeable pile-up effect did exist. Figure 18 shows a similar pulser test for Co-59, with the same parameters for detector-amplifier system as were employed in the previous experiments. As you can see the effect is too small to be observable here, because of the much lower counting rates. While this is true for the important Co-59 and U-238 experiments, it does seem clear that the extensive interference analysis done for gold, by the BNL group, are subject to pile-up distortions and must be corrected.

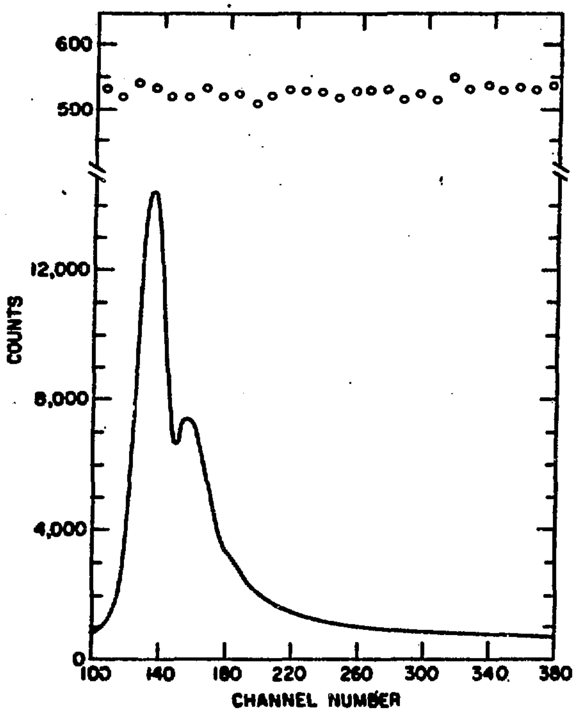

Fig. 18 Counting rate losses in Co-59 near the 132 eV resonances.

In summary, the direct capture amplitude has been convincingly demonstrated for a few target nuclides like Co-59 and U-238. Within the large errors and inevitable ambiguities of these experiments, the results are in accord with the simple hard-sphere capture estimates of Lane and Lynn. Not enough data are available to check the intermediate coupling model. It would be desirable to do so near the 3s and 4s giant resonances.

III. CORRELATIONS AND THE STATISTICAL PROPERTIES OF RADIATIVE WIDTHS

The extraction of partial radiative widths from resonance spectral data is not a completely straightforward process. As previously stated, the assumption must be made that the capturing rate is proportional to the total detector response, integrated over all pulse height ranges. Some groups have chosen to normalize to the intensities of a few low energy lines. In either case, one <u>assumes</u> that the branching ratio is given by an expression of the form:

$$\Gamma_{\gamma f}/\sum_f \Gamma_{\gamma f} = k\ ^{A(\text{peak } f)}/\text{capture rate}$$

and one assumes a negligible variation of $\Gamma_\gamma = \sum_f \Gamma_{\gamma f}$ from resonance to resonance. Neither of these assumptions is completely valid, but at the same time neither is expected to depart from the assumption by more than about 20%. For example, in a medium to heavy nucleus $\langle\Gamma_{\gamma f}\rangle/\Gamma_\gamma \approx 0.01$ and, assuming a Porter-Thomas width distribution

$$\left(\frac{\delta\Gamma_\gamma}{\Gamma_\gamma}\right)^2 \approx 0.02;\ \frac{\delta\Gamma}{\Gamma} \approx 14\%.$$

In a resonance experiment it is frequently possible to compare branching ratios $(\Gamma_{\gamma f}/\Gamma_\gamma)$ with the intensities measured at thermal, and use previously measured thermal capture intensities. Alternatively it is possible to intercompare resonances of different nuclides and measure all partial widths relative to one standard transition. Following a suggestion of Carpenter [33], we can write for the capture rate in a resonance:

$$Nc = (1+\Gamma_n/\Gamma)\int\Phi(E)[\sigma_\gamma(E)/\sigma(E)](1-e^{-n\sigma(E)})dE$$

where the factor $(1+\Gamma_n/\Gamma)$ approximately includes the effect of scattering before capture. The most commonly used standard at present is gold, since the capture rate in gold may be accurately inferred from counting the 412 keV γ-ray from Pt-198, following β decay from Au-198. Thus the comparison of a high energy γ-ray with the 412 keV, after a small correction for internal conversion, and after suitable corrections for detector efficiency as a function of energy [34], results in an absolute photon intensity. Furthermore the gold spectrum has been accurately measured from thermal to 5.0 eV by Walter Kane, with the BNL neutron monochromator. The following table of resonance and thermal intensities has been provided by Kane:

TABLE III: $^{197}Au(n,\gamma)^{198}Au$ Absolute Intensities

(photons per 1000 captures)

E_γ	Thermal	4.9 eV
6513	16.4	14.9
6457	22.5	25.3
6320	34.5	27.0
6276	11.5	12.1
6264	2.4	1.4
6252	56.9	52.6
6165	1.7	0.2
6149, 6145	12.0	8.3
6106	5.6	9.4
Sum	163.6	151.2

The 4.9 eV intensities are currently being used in determining the absolute resonance intensities at BNL, and with the assumption of constant radiation width, the absolute partial widths may be derived.

The significance of the distribution and statistical properties of the partial widths has been summarized by Lane [35]. The quantitative embodiment of the Bohr theory of the compound nucleus, carried to its extreme statistical form lies in two assumptions:

1) $\sum_{\gamma} \gamma_{\lambda c}\gamma_{\lambda c'} = 0$, where $\gamma_{\lambda c}$ is the partial width amplitude for channel c, and

2) $\frac{1}{\Delta E} \sum_{\lambda} \gamma^2_{\lambda c}$ = Sn is energy independent.

These sums are taken over an energy region covering many resonances λ. The omission of levels outside the region ΔE implies a negligible background from distant levels. The values of $\gamma^2_{\lambda c}$ for medium to heavy nuclei are in the order of 10^{-7} of single particle width. If we therefore expand the compound resonance wave function in terms of products of channel states and excited states of the core nucleus, we would expect in the order of 10^7 terms in the expansion. An intuitive corollary of this statement of complexity is that the $\gamma_{\lambda c}$ are, by the central limit of statistics, distributed about zero in Gaussian fashion. The widths $\Gamma_{\lambda c} = 2P_c\gamma^2_{\lambda c}$ are therefore distributed in a χ-square distribution with $\nu = 1$, the well-known Porter-Thomas distribution. For radiative transitions, we assume the energy independence of the reduced matrix elements, implying that the partial radiative widths, on the average, vary with γ-ray energy according to the phase space factor E^3.

From the extreme statistical model we get no direct capture and no width correlations. Lane has shown that width correlations and direct capture are intimately related

From R matrix theory:

$$Rcc'(E) \equiv \sum_{\lambda} \frac{\gamma_{\lambda c}\gamma_{\lambda c'}}{E_{\lambda}-E}$$

$$\text{Im } Rcc'(E^+) = \pi\gamma_{\lambda c}\gamma_{\lambda c'}/D; \quad E^+ = E + i\epsilon \quad \epsilon >> D$$

then
$$\rho(\gamma_{\lambda c}, \gamma_{\lambda c'}) = \frac{\sum_{\lambda}\gamma_{\lambda c}\gamma_{\lambda c'}}{\sqrt{\sum_{\lambda}\gamma^2_{\lambda c}\sum_{\lambda}\gamma^2_{\lambda c'}}} = \frac{\text{Im } Rcc'(E^+)}{\sqrt{\text{Im } Rcc(E^+)}\sqrt{\text{Im } Rc'c'(E^+)}}$$

and
$$\text{Re } Rcc'(E^+) = \frac{1}{\pi} \int \frac{\text{Im } Rcc'(E^+)dE'}{E'-E}$$

$$\sigma(\text{direct}) \propto |Rcc'(E^+)|^2$$

$$\sigma(\text{background}) \propto [\text{Re}Rcc']^2$$

The situation where $\rho \approx 1$ implies that $\gamma_{\lambda c}$ and $\gamma_{\lambda c'}$ behave the same in a range of λ; namely that there is a single state d for which

$$\gamma_{\lambda c} = \langle \lambda | d \rangle \gamma_{dc}$$

$$\gamma_{\lambda c'} = \langle \lambda | d \rangle \gamma_{dc'}$$

This situation Lane refers to as a common doorway for the channels c,c′. In this case the real and imaginary parts of $R_{cc'}$ are of the same order of magnitude and that the non-resonant cross section is closely related to the correlations:

$$\sigma_{cc'}(\text{non resonant}) = \rho(\Gamma_{\lambda c},\Gamma_{\lambda c'})\sigma_{c(abs)}\frac{\bar{\Gamma}_{\lambda c'}}{D}\frac{\pi}{2}\left(\frac{ReR_{cc'}}{ImR_{cc'}}\right)^2$$

$$\sigma(abs) = g\frac{2\pi^2}{k_c^2}\frac{\bar{\Gamma}_{\lambda c}}{D}$$

The detailed verification of this formula has not been achieved, however, because of a lack of sufficient data on non-resonant cross sections. We shall return to this point later.

The non-statistical effects observed experimentally fall into three classes:

1) structure in the photon spectrum, observed both in (n,γ) and (d,p) cross sections. First observed by Groshev, and Bartholomew and his collaborators, and by Berqvist and Starfelt for fast neutron capture [36], the structure or bump is interpreted as due to the presence of 2 particle-1 hole doorway states

2) correlations of (n,γ) and (d,p) strengths. These are seen in thermal and resonance (n,γ) studies. They are large in the region $A < 100$ and small for $A > 100$.

3) correlations between partial radiative widths and neutron widths.

The simplest and most dramatic example of 2) and 3) was reported by the BNL group about one year ago, in the molybdenum isotopes 92 and 98 [37]. This example is one of the simplest common doorway--that consisting of a product $u_\ell\Phi(o)$ where u_ℓ represents the incident neutron's wave function with orbital angular momentum ℓ and $\Phi(o)$ is the unexcited core's wave function.

This common doorway is just the valence model described by Lynn [21]. In this model the radiation results from the single particle motion of the added neutron in the presence of the ground state of the target.

The experimental evidence for this startling effect is displayed concisely in Fig. 19, obtained for four resonances in Mo-98 with the Brookhaven fast chopper, at 429, 467, 612, and 818 eV. Three of the 4 show strong transitions in the region from 5-6 MeV. These are p-wave resonances with exceptionally large p-wave reduced widths. The 467 eV s-wave resonance shows a spectrum characteristically lacking in high energy lines. The qualitative similarity of the 429 and 612 eV is readily apparent. What may not be so apparent is the fact that the 818 eV resonance spectrum is simply explained by the fact that the resonance is a p-3/2 level as contrasted to the p-1/2 resonances at 429 and 612 eV. That the Porter-Thomas distribution does not hold is clear from the behavior of the ground state transition.

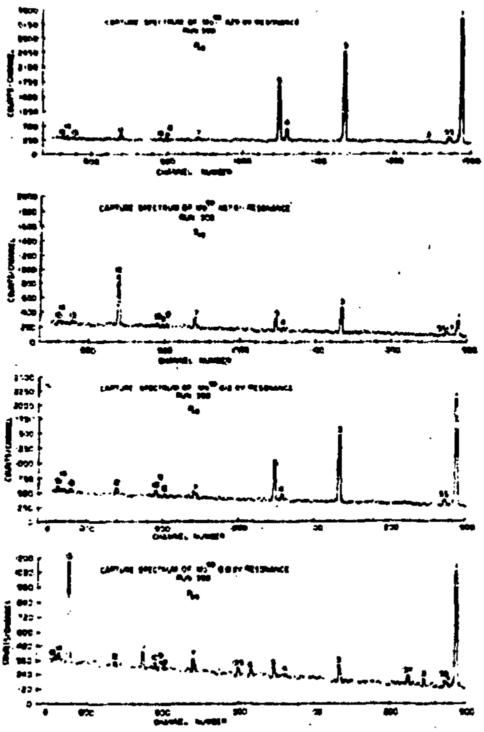

Fig. 19 Four resonances in Mo-98. The p-1/2 429 eV, the s-1/2 467 eV, the p-1/2 612 eV and the p-3/2 813 eV.

Mo^{98} and Mo^{92} in simplest terms can be considered closed shell nuclei. N = 50 for Mo-92; for 98 the d-5/2 shell is filled. The low lying levels of Mo-99 and Mo-93 have, accordingly, large spectroscopic factors--e.g. 0.67 for the 1/2 ground state of Mo-99. The formula for the valence neutron transition model, that is ascribing the radiation as due only to the single particle neutron motion, is as follows [21]:

$$\Gamma_{\lambda\mu} = \frac{16\pi k^3}{9}\, \theta_\lambda^2 \theta_\mu^2 \left|\bar{e}\int_0^\infty dr\, u_\lambda r\, u_\mu\right|^2 \times \frac{|\langle j'IJ_\lambda||Y^{(1)}||j''IJ_\mu\rangle|^2}{(2J_\lambda+1)}$$

where

$$\frac{|\langle j'IJ_\lambda||Y^{(1)}||j''IJ_\mu\rangle|^2}{2J_\lambda+1} = \frac{3}{4\pi}(2J_\mu+1)(2j'+1)(2j''+1)(2\ell'+1)$$

$$\times\, W^2(j'J_\lambda j''J_\mu;I1)$$

$$\times\, W^2(\ell'j'\ell''j'';\tfrac{1}{2}1)$$

$$\times\, C^2_{\ell'1}(\ell'0;00)$$

This formula is strikingly successful when applied to the p-3/2→s-1/2,d-3/2, d-5/2 and p-1/2→s-1/2,d-3/2 transitions in the molybdenum isotopes, especially when the dimensionless reduced widths $\theta_\lambda^2 = \gamma_\lambda^2/(\hbar^2/ma^2)$ and $\theta_\mu^2 = \gamma_\mu^2/\hbar^2/ma^2)$ are large. The comparison between predicted and measured widths is given in Fig. 20, and the photon intensities in Table IV.

TABLE IV: The γ-ray intensities, in photons per 10^3 captures, recorded for p-wave resonances of Mo-98

			1 Mo^{98} P-wave Resonances						
		Γ_n^1(eV)	.37±.04	3.17±23	1.11±16	1.78±.56			
Peak #	E_γ,keV	E_x keV/E_n, eV	$P_{3/2}$ 12eV	$P_{1/2}$ 429eV	$P_{1/2}$ 612eV	$P_{3/2}$ 818eV	S(d,p)	J^π	ℓ
1	5926.9	0	31.3±2.4	201±10	188±15	186±10	0.67	1/2+	0
2	5829.4	97.5	1.2±0.6	3.7±1.5	0.5±0.5	6.7±1.2	0.21	5/2+	2
3	5575.9	351.0	22.3±2.3	138±5	111±5	26.0±2.0	0.11	3/2+	2
4	5400.9	526.0	1.2±0.6	20.0±1.4	16.0±4.5	5.2±1.0	.042	1/2+	0
5	7379.1	547.8	28. ±1.8	91.5±4.3	64.1±3.4	18.3±4.1	0.43	3/2+	2
6	5310.9	616.0	0.6±0.6	1.9±0.5	1.9±1.0	12.7±2.5	.018	5/2+	2

The agreement is not only qualitative, but quantitative. If we convert the photon intensities to partial widths by assuming a radiation width total of:

$$\Gamma_\gamma = 145 \text{ meV} + \delta\Gamma$$

where $\delta\Gamma$ is computed by summing over all transitions with significant strength, then the agreement with the model is about 20%, on an absolute basis, with the valence model. Closer inspection of the figure, however, will show somewhat better agreement for p → s transitions than for p-d.

If one bears in mind the fact that these molybdenum isotopes are at the 3p single particle resonance, and that the reduced widths of these p-wave levels are abnormally large, it is perhaps not surprising that valence neutron effects are significant.

Recently the molybdenum work has been extended to higher neutron energies through use of the ORELA facility. The spectra obtained at higher energies confirm the non-statistical behavior of neutron capture; detailed comparison with the model, however, is difficult because of a lack of knowledge of the resonance spins and neutron widths. Transmission measurements are now in progress to permit a more detailed examination of the effects. Part of the picture is shown in the following figures [38].

A comparison of relative intensities of the spectra for the p-3/2 molybdenum-92 resonances at 5.6 and 12.8 keV with the valence model shows excellent agreement, Fig. 21. The spectrum of the 23.9 keV p-1/2 resonance is compared to the prediction in Fig. 22. Some other spectra, however, do not

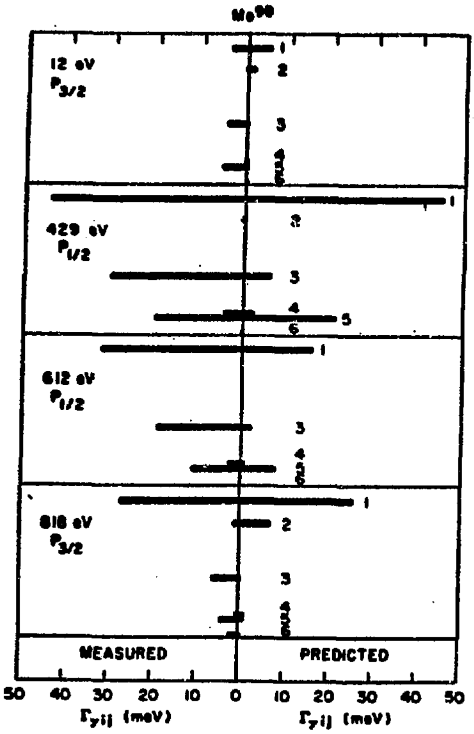

Fig. 20 The comparison of Mo-98 widths with the valence model predictions.

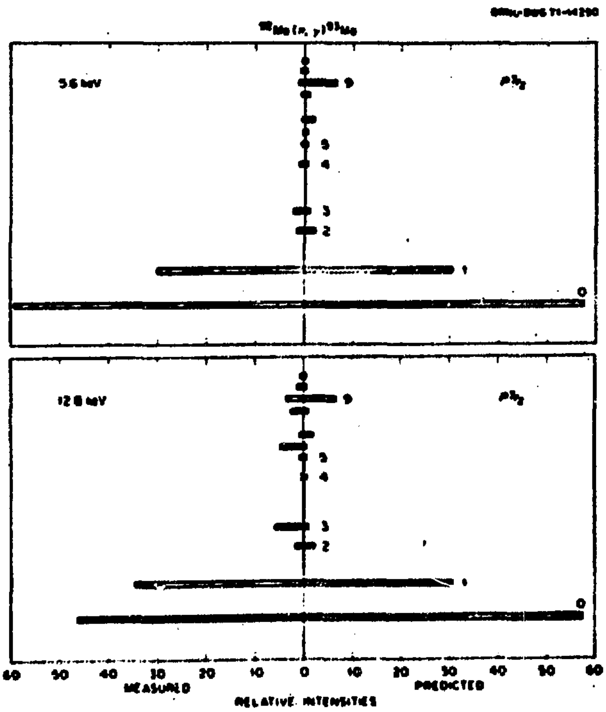

Fig. 21 The 5.6 and 12.8 keV Mo-92 resonances compared to valence model predictions.

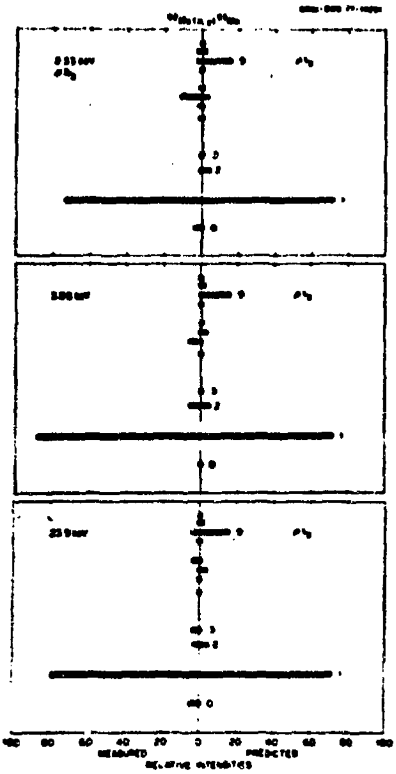

Fig. 22 The 23.9 keV p-1/2 resonance spectrum compared to the valence model prediction. Spectra from the 2.33 keV p-3/2 (?) and 3.06 keV p-1/2 resonances are also shown.

show as good agreement as the above. For example the three p-1/2 resonances at 4.3 6.8, and 7.1 keV are examples of relatively poor fits to the model. The conclusions based on these qualitative arguments are the following:

1) The strong appearance of the 7129 keV γ-ray, to the first excited state, for 16 of the 19 p-wave resonances, violates the hypothesis of purely statistical decay, and

2) 5 of the 19 resonances are in excellent agreement with the valence model.

Further conclusion awaits completion of the measurements of neutron widths from transmission experiments.

The valence affect, observed in molybdenum, poses a problem for theoretical interpretation: we know that giant E-1 resonance absorbs the major part of E-1 strength from the uncoupled single-particle transitions near 7 MeV. Why do particular transitions have their strengths unaffected by the redistribution? Why do such transitions correspond to states lacking core excitations?

According to Lane [19], unpublished calculations by Soper for closed shell nuclei Ni-60 and Pb-208 using zero-range forces, indicate that after diagonalization of the 1p-1h states a significant amount of E-1 strength is left at low energies and this component is associated with $p^{-1}s$ neutron components. This amount is about 4% of the total E-1 strength in Ni-60.

As for the second point, Lane has hypothesized that the 3p state in the threshold region has an anomolously small spreading width. This results from the specific property of the 3p state near threshold that a large fraction of the wave function lies in the external region. The mixing with neighboring 3p functions coupled to excited states of the core is estimated to be reduced from ~ 3 MeV to about 0.7 MeV, and the mixing with other 3p states diminished by the square of the reduction factor in spreading width.

Correlations of the valence model type might reasonably appear to be associated with the strength function peaks, and some evidence for them has reported near the 3s and 4s giant resonances. An example of a possible effect has been reported by Block, Steiglitz, and Hockenbury [39] for capture widths in isotopes of Cr, V, and Ni. The measurements were performed with a total energy detector--a liquid scintillator tank. For these nuclides the bulk of the total capture width is contained in a few transitions. Block, Steiglitz, and Hockenbury observe significant correlations between reduced neutron widths and radiative widths on a sample of 27 resonances from Cr-50, 52, 53, 54, Ni-60, and vanadium. The linear correlation coefficient $p(\Gamma_n^o,\Gamma_\gamma)$ for these 27 resonances is 0.47. For the 12 resonances formed from the doubly even target nuclei Cr-50, 52, 54 and Ni-60, the coefficient is 0.80. No individual measurements of partial widths have been made, but in the inverse photoneutron experiment, Jackson has examined the corresponding resonances in Cr-53 and Ni-61, and derived the correlation coefficients between reduced neutron width and ground state radiation width [40]. Jackson does not find a large correlation (0.39 for 12 resonances in Ni-61 and 0.04 for 7 resonances in Cr-53). The effect is thus not a simple valence transition since it appears not to occur for the ground state transition, which generally has a sizeable reduced width.

In the 4s giant resonance correlations between neutron and radiative widths might be expected to be weaker because of the greater fragmentation of single particle strength among the final states. In Dy-163, the BNL group reported a positive correlation for a number of transitions between radiative widths and neutron reduced widths [41]. From 17 resonances, and averaged over five low-lying states a correlation of 0.35 was measured for J=3 resonances. The eight J=2 resonances do not exhibit significant correlations. Plots of two of these transitions are given in Fig. 23. Additional resonances are to be included to increase statistical sample size in experiments being carried out at ORELA.

A weak, but significant correlation was reported several years ago in Tm-169 by groups at Brookhaven and Argonne [42,16]. The average correlation, based on 8 J=1 resonances and averaged over 15 final states, was $\langle\rho\rangle = 0.274$. This correlation resulted largely from the strong transitions present in the 3.9 eV resonance, which has a larger-than-average neutron reduced width. In subsequent experiments the precision of this coefficient was improved by increasing the sample size, and the incorrect spin assignment of the 153 eV J=0 resonance was corrected (see ref. 19). The result of these subsequent corrections is that this correlation is in fact not significantly different from zero; for 24 J=1 resonances averaged over the same 15 final states as the earlier experiments, $\langle\rho\rangle = +0.046\pm.06$ is obtained. The influence of the 3.9 eV resonance is diluted as additional resonances are added to the sample.

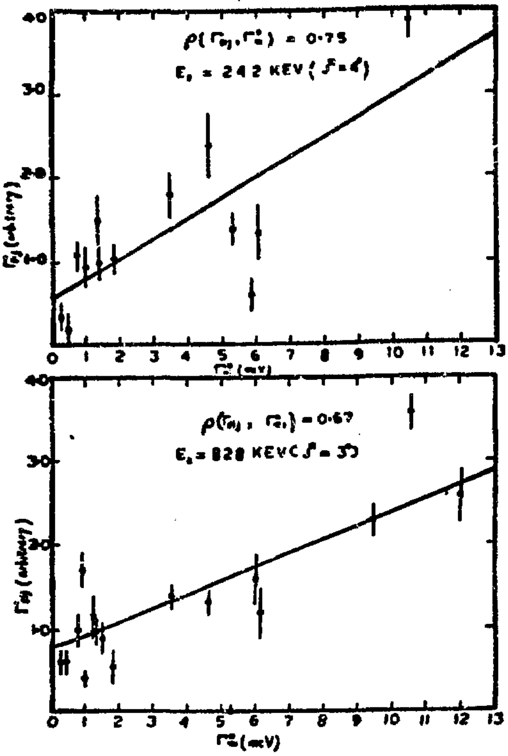

Fig. 23 A demonstration of correlation between reduced neutron width and partial radiative widths for two transitions in Dy-163.

It is interesting to review the experimental situation in U-238 resonance partial widths in view of the significant direct capture cross section deduced from the resonance-direct interference analysis in U-238. Recently a collaborative experiment between BNL and Oak Ridge was performed to establish the statistical properties of the partial widths [43]. In this experiment the γ-rays spectra from 28 resonances in U-238 were recorded at ORELA. Certain features of the experiment are noteworthy.

The distribution of partial widths in U-238 is in satisfactory agreement with the Porter-Thomas hypothesis. The number of degrees of freedom for each of the 15 most intense γ rays is shown in Fig. 24. The result for 12 of the 15 γ rays (a complex group near 4065 is omitted), normalized to unit mean for each transition is as follows:

$$\nu = 1.20\,^{+0.20}_{-0.15}, \text{ for 23 resonances in U-238.}$$

Although several individual transitions fall outside 10 to 90° confidence limits--the 3583, 4060, and 4067 keV γ-rays--this fact is not unusual for a sample of 15.

Of interest is the possible width correlations in U-238, in the light of what was previously indicated about the connection between width correlations and direct capture. The direct capture component of >1.8 mb at 1 eV found from previous experiments for the 4060 keV γ-ray, would from Lane's formula,

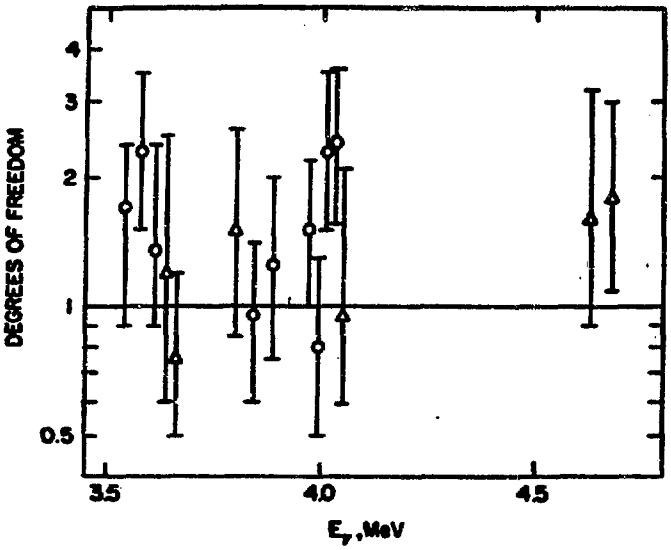

Fig. 24 Distribution parameters ν for high energy transitions from U-238(n,γ)U-239.

predict a sizeable correlation between neutron width and radiative width for this transition, if the real and imaginary parts of the R function are comparable: for $D = 20$ eV, $\Gamma_{\gamma i} \approx 200$ μeV, $\sigma(D) = 2$ mb and $\sigma_{abs} \approx 400/\sqrt{E}$, then $\rho \approx 0.3$.

The experimental correlation however is consistent with zero, indicating that the distant level contribution to the background cross section is fairly small, and that ReRcc′ << ImRcc′.

Apart from the following anomalous results, the U-238 measurement is thus consistent with the statistical picture:

1) A direct reaction component of $\sim$ 2 mb (evaluated at 1 eV)

2) An anomalous correlation between the intensities of the 3991 keV and 3982 keV γ-rays

3) A rather high value for the M-1 strength function

$$k \equiv \frac{\Gamma_\gamma(\mathrm{eV})}{E^3(\mathrm{MeV})\,D(\mathrm{eV})} = 25.6 \pm 5.1\times10^{-3}$$

IV. INTERMEDIATE STRUCTURE IN THE PHOTON STRENGTH FUNCTION

The extreme statistical model for radiative decay, as normally conceived, allows for no energy variation in the radiative matrix elements beyond the phase space factor: k^{2L+1}.

For dipole transitions, therefore, a E^3 energy dependence is expected.

We know, however, that the extreme picture cannot be correct. The well known electric dipole giant resonance, peaked in the region from 15-25 MeV for most nuclei, implies a severe energy dependence. Axel pointed out that this concentration of intensity could have an influence down to the region of the neutron binding energy, 6-8 MeV [44]. Rosenzweig proposed the plausibility of assuming a giant resonance based not only on the ground state, but each nuclear excited state [45]. Under this assumption, the energy variation is exhibited by studying the photon energy spectrum, where transitions are initiated at a single or narrow band of energies, and terminate on many final states.

For the testing of the Axel-Rosenzweig hypothesis the average capture method of Bollinger is ideal, for it provides an averaging over the statistical fluctuation--and non-statistical effects--which might mask the energy variation.

The giant dipole resonance is assumed to be describable by a Lorentzian function of the form:

$$\frac{\langle\Gamma_{if}\rangle}{D} = E_\gamma^4\left[\frac{\sigma_a^o\Gamma_a^2}{(E_a^2-E_\gamma^2)^2+E_\gamma^2\Gamma_a^2}\right]$$

where the subscript a refers to the giant resonance position and σ_a^o, Γ_a are its parameters, determined from photonuclear reactions. In the application of the average capture method, a further complication must be dealt with; namely the various channel spins in the reaction. Figure 25 illustrates the results of the technique for Ho-165 [11]. The relative intensities of the observed transitions are plotted as I/E_γ^3, and appear in broad bands. For Ho-165 the channel spins are 3 and 4, and from statistical considerations the final states 3^+ and 4^+ should be populated with twice the intensity of the 2^+ and 5^+ states. This conception is largely borne out by the figure. Furthermore the general tendency of the transitions to vary with energy more strongly than E^3 is indicated by the sloping lines on the figure. Bollinger has concluded, from such evidence, that the energy variation is more nearly E^5, in accord with the extrapolation of the giant resonance.

In principle the average spectrum method could be used to resolve related questions often raised about photon strength functions: for example, is there a "pygmy" E-1 resonance, as suggested by Bartholomew and his collaborators? And what is the evidence for an M-1 resonance? The average spectrum method in principle may also reveal nuclear structure effects in the (n,γ) reaction, in explicitly exhibiting a possible dependence of the transition probabilities on the structure of the final states of the residual nucleus. Two problems, however, limit the effectiveness

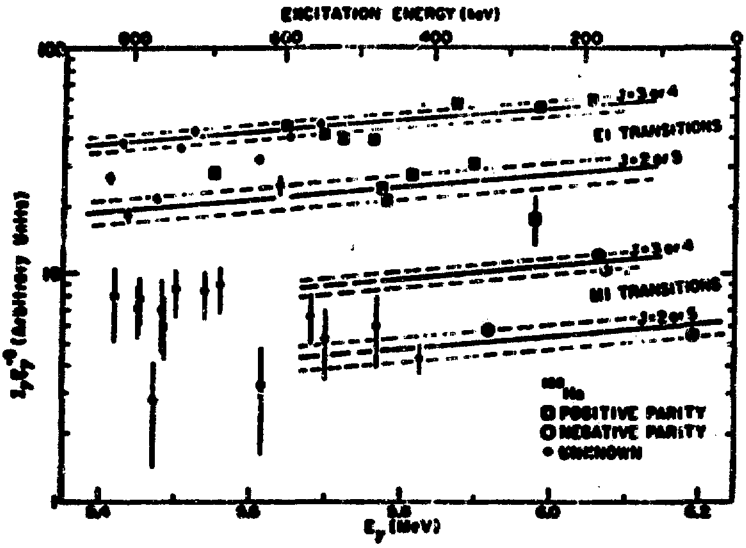

Fig. 25 The energy variation of γ-ray intensities from H-165(n,γ)Ho-166.

of the method: 1) its non-selective character, and 2) inefficiency in averaging. Since there is no selectivity in the capturing states possible, the resulting spectrum unavoidably contains contributions from many resonances of varying spins, parities, and sizes. Some information can be gleaned from a detailed inspection of γ-ray line shapes--p-wave capture, for example, is associated with the broader components of the incident neutron spectrum and therefore manifests itself as an increased high energy tail on the γ-ray transition peak. Such a detailed inspection of peak shape is difficult to apply in a complex spectrum where closely spaced peaks are difficult to separate. On the other hand, for many nuclides the available spectrum is not wide enough to permit sufficient averaging--for 100 levels the root-mean-square averaging error is 14%. Hence nuclear structure effects of this size would not be readily apparent.

The "pygmy" E 1 resonance near 5.5 MeV has been suggested as a possible example of doorway states by Bartholomew and his co-workers [46]. The effect has been known for some time, from the spectral distributions obtained by Groshev and co-workers in thermal (n,γ) work. As seen in Fig. 26, where the effect is given as measured by a low-resolution NaI(Tℓ) detector, the "pygmy" resonance is manifested as a bump in the spectrum. The bump is evident in the region just below the N=126 shell closure, from thallium (Z=81) down to tantalum (Z=73), where it disappears.

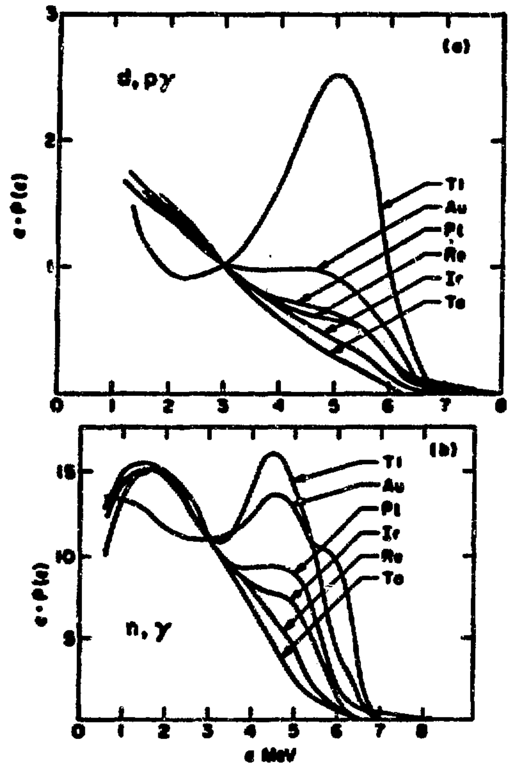

Fig. 26 Evidence for a pygmy E-1 resonance from (n,γ) and (d,p) experiments.

Bartholomew demonstrated that the bump consisted of mostly E-1 transitions in the case of Hg-200; hence an explanation in terms of M-1 spin flip transitions cannot be tenable [47]. The bump is also seen in fast neutron capture [36] and in the (d,p) experiments [46], and from these experiments it is certain that the bump is not a function of excitation energy. This fact led Bartholomew to propose a mechanism in which the radiation is emitted as a γ-ray decay from a 2p-1 hole doorway state. In Lane's terminology the 2p-1 hold state would be a common doorway for the neutron and photon channels. In support of this hypothesis are experiments on the inelastic scattering of neutron capture γ-rays from Tl-205, Tl-203, W, and Bi by Moreh and collaborators [48]. They find, in addition to elastically scattered γ-rays, other strong lines near 5.5 MeV. Moreh invokes the same mechanism as that proposed by Bartholomew.

This effect should be observable near other shell closures. The BNL group report a similar effect near the N=50 shell closure [49]. In this case, however, the capture of p-wave neutrons is involved. The p-wave levels in Nb-93 are characterized by strong high energy transitions, as compared to the s-waves. The energy averaged spectra are shown in Fig. 27, where a "bump" in the p-wave spectrum shows up near 6.5 MeV, and this bump is absent for the s-wave spectra. The low-lying states in Nb-94 are mostly S and D states, and these are strongly populated in both (d,p) and (n,γ) experiments, as shown in Fig. 28. An (n,γ), (d,p) correlation coefficient of +0.578 is found, with a significance level of better than 99.9%. Proton particle-hole

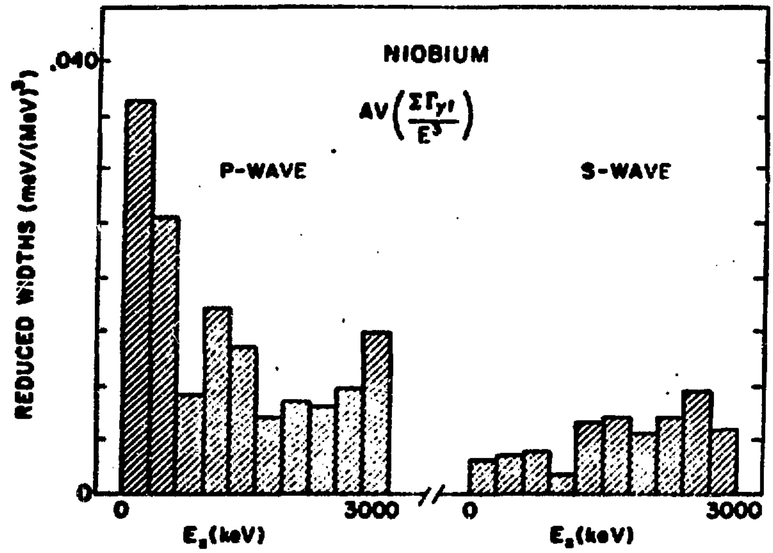

Fig. 27 The energy-averaged spectra for p- and s-wave Nb-93 resonances.

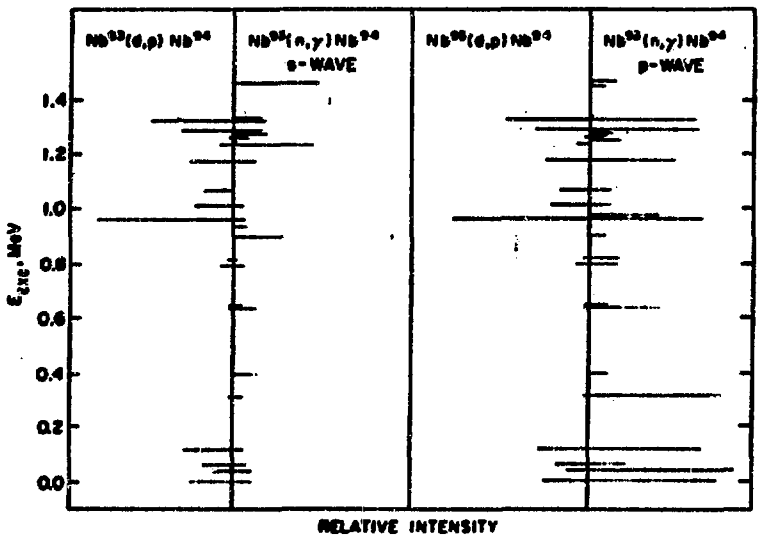

Fig. 28. Averaged (over resonances) partial radiative widths from Nb-93 compared with (d,p) cross sections.

states are available near N=50: 3s-1/2→2p-1/2,3s-1/2→2p-3/2 2d-5/2→1f-5/2, and the incident neutron could be left in a ℓ=2 or ℓ=0 state. In this situation we must hypothesize a number of overlapping doorway states, in which case the correlation between neutron and radiation widths is reduced by the factor 1/n, since the experimental $\Gamma_n^0,\Gamma_{\gamma f}$ correlation is not significant.

Another sensitive method for determining structure in the energy dependence is afforded by the threshold photoneutron technique. A series of experiments carried out by Bowman and his colleagues at Livermore, by H. E. Jackson at Argonne, and the Harwell group have examined the question of the distribution in photon strength by observing the photoneutron yields.

Their general conclusion is that the ground state radiation strength is not distributed statistically among resonances. Definite indications of concentration in narrow energy regions are observed and interpreted as indications of intermediate structure. Let us examine a few examples.

a) Fe-57. Jackson reports an anomalous concentration of strength in the $3/2^-$ doublet at 230 keV, clearly inconsistent with a statistical distribution [19]. He attributes this effect to a large admixture of the configuration $f_{5/2}f_{7/2}^{-1}$ particle-hole pair coupled to the Fe-57 ground state. The spin-flip transition mechanism suggested by Mottelson is perhaps responsible for the M-1 enhancement. Jackson also finds an anomalously strong resonance with spin $1/2^-$ near 600 keV, which is interpreted as the corresponding recoupling of the particle-hole pair. A similar effect has been noted in Cr-53.

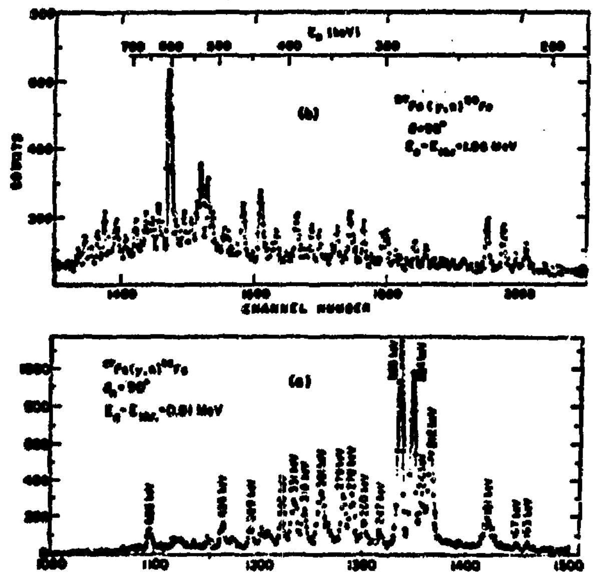

Fig. 29 Photoneutron spectra from Fe-57(γ,n)Fe-56, taken with a proton recoil detector at higher energies, and a Li-6 detector at lower energies.

b) Pb-207. Berman, Baglan, and Bowman find the pattern of ground state γ-ray widths from $1/2^+$ levels in Pb-207 (γ,n) which correlates qualitatively the pattern of reduced neutron widths in Pb-206 (n,n) [19]. In distinction to the case in Fe-57, this is cited as a common doorway in photon and neutron channels, in which case the widths are expected to correlate.

c) Pb-208. A concentration of M-1 strength is found by Berman et al. in 1^+ resonances near 400 keV [19]. The total γ-ray strength is found to be 50.8 eV, more than 5 Weisskopf units and at least half of the total M-1 strength for Pb-208. The origin is thought to be spin flip transitions from the $i_{13/2}$ neutron shell and $h_{11/2}$ proton shell.

d) Winhold et al. have measured photoneutron yields in Sn-119 and Sn-117 and found broad peaks, several hundred keV wide at 7.8 MeV in each isotope[50]. These peaks were not identified as to parity, but if they were $1/2^+$ in character, they could be ascribable in terms of a $g_{9/2} \rightarrow g_{7/2}$ proton transition, as expected in the tin isotopes.

e) Si-29. A recent experiment by Jackson has been performed on the isobaric analog of the $1/2^+$ first excited state of Al-29 [51]. This appears near 1093 keV above the neutron separation energy in Si-29. Figure 30 shows a comparison of the reduced neutron widths derived from the corresponding Si-28 (n,n) reaction with the ground state radiation widths derived from Si-29 (γ,n). The correlation is striking and has a value of +0.88.

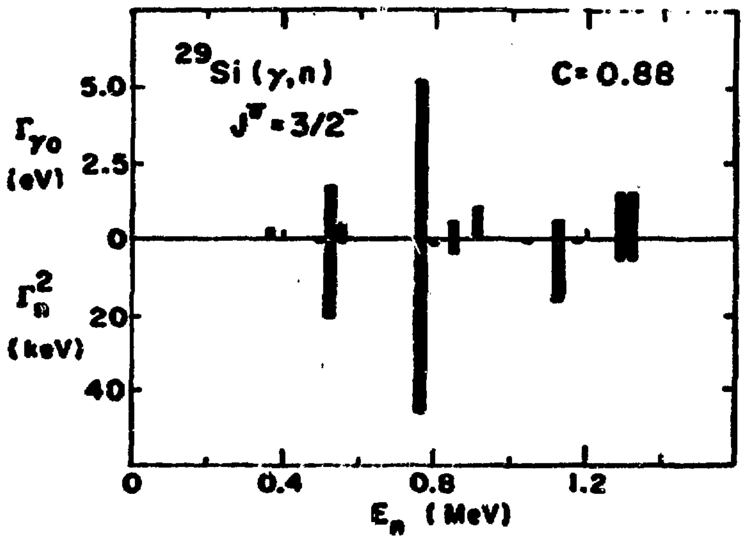

Fig. 30 Evidence for a common doorway in Si-29(γ,n)Si-28.

A survey of these photoneutron data produces the inescapable conclusion that the radiation strengths are not distributed in a statistical manner. The anomalous concentrations of M-1 strength are clearly associated with spin-flip transitions, and indicate that simple nuclear structures appear as important components in wave functions of highly excited states.

CONCLUSION

This review of nuclear structure effects in neutron resonances has been necessarily incomplete. Many interesting aspects of current work have been omitted. We have not discussed, for example, intermediate structure in resonances below the fission thresholds. Neither have we attempted to describe some interesting directional correlation studies which are invaluable in assigning resonance spin and parities. (Currently the BNL group is studying directional correlations between the neutron beam and emitted photon in the p-wave resonances in niobium. The technique is able to measure the amount of channel spin component in various resonances.) The attempt has been to summarize some of the interesting facets of neutron resonance spectroscopy, especially in the radiative decay of resonances, and to give some idea of the richness of this field. Many mysteries remain to be solved; many discrepancies remain to be resolved. The result of these solutions and resolutions will be a clearer picture of the structure of these highly excited metastable states.

The author is indebted to H. E. Jackson, Walter Kane, G. W. Cole, O. A. Wasson, and G. G. Slaughter for prior communication of material to be published; and to useful discussions with M. R. Bhat and S. F. Mughabghab. E. R. Reddingius provided valuable information on the status of polarized γ-ray experiments.

REFERENCES

[1] J. Chadwick, Proc. Royal Soc. A136, 692 (1932)
[2] J. R. Dunning, G. B. Pegram, G. A. Fink, D. P. Mitchell, and E. Segré, Phys. Rev. 48, 704 (1935)
[3] F. G. P. Seidl, D. J. Hughes, H. Palevsky, J. S. Levin, W. Y. Kato, and N. G. Sjostrand, Phys. Rev. 95, 476 (1954)
[4] W. H. Zinn, Phys. Rev. 71, 752 (1947)
[5] E. Fermi, E. Amaldi, O. D'Agostino, F. Rasetti, and E. Segré, Proc. Royal Soc. (London) A146, 483 (1934)
[6] D. E. Lea, Nature 133, 24 (1934)
[7] R. C. Greenwood and W. W. Black, Phys. Letters A21, 702 (1966)
[8] L. V. Groshev, A. M. Demidov, V. N. Lutsenko, V. I. Pelekhov, Izvest. Akad. Nauk SSSR, Ser. Fiz. 26, 979 (1962) (as quoted by L. M. Bollinger, ANL Informal Report PHY-1970C)
[9] R. E. Chrien and M. Reich, Nucl. Instr. and Meth. 53, 93 (1967)
[10] W. R. Kane, Phys. Rev. Letters 25, 953 (1970)
[11] L. M. Bollinger and G. E. Thomas, Phys. Rev. C2, 1951 (1970)
[12] M. A. Betz, J. W. Reynolds, and G. G. Slaughter, CONF 690301, Columbia U., New York (1969)
[13] O. D. Simpson and L. G. Miller, Nucl. Instr. and Meth. 61, 245 (1968)

[14] B. W. Howes, R. M. Brugger, J. W. Rogers, R. P. Schuman, F. B. Simpson, and O. D. Simpson, IN-1308 Idaho Nuclear Corporation, Idaho Falls, Idaho (1969)
[15] H. T. Motz, Neutron Capture Gamma-Ray Spectroscopy, Ann. Rev. Nucl. Sci. 20, 1-38 (1970
[16] L. M. Bollinger, Nuclear Structure: Dubna Symposium,IAEA, Vienna 1968, p. 317
[17] R. E. Chrien, Neutron Capture Gamma-Ray Spectroscopy (Studsvik), IAEA, Vienna 1969, p. 627-648
[18] G. A. Bartholomew, Neutron Capture Gamma Rays, Ann. Rev. Nucl. Sci. 11, 259-302 (19621
[19] J. B. Garg, Editor, Statistical Properties of Nuclei, Plenum Press, New York-London, 1972
[20] A. M. Lane and R. G. Thomas, Rev. Mod. Phys. 30, 257 (1958)
[21] J. E. Lynn, "The Theory of Neutron Resonance Reactions", Clarendon Press, Oxford (1968)
[22] A. M. Lone and J. E. Lynn, Nucl. Phys. 17, 563; 586 (1960)
[23] L. V. Groshev, A. M. Demidov, V. N. Lutsenko, and V. I. Pelekhov, Proc. Int'l Conf. Peaceful Uses Atomic Energy, 2nd, Geneva 15, 138 (1958)
[24] R. E. Chrien, D. L. Price, O. A. Wasson, M. R. Bhat., M. A. Lone, and M. Beer, Phys. Letters 25B, 195 (1967)
[25] O. A. Wasson, M. R. Bhat, R. E. Chrien, M. A. Lone, and M. Beer, Phys. Rev. Letters 17, 1220 (1966)
[26] R. K. Sheline, W. N. Shelton, T. Udagawa, E. T. Jurney, and H. T. Motz, Phys. Rev. 151, 1011 (1966)
[27] G. F. Auchampaugh, UCRL 50504 (1968)
[28] K. Abrahams, J. Kopecky, F. Stecker-Rasmussen, Phys. Letters 32B, 605 (July 1970)
[29] J. Honzatko and J. Kajfosz, as quoted by E. R. Reddingius
[30] C. D. Bowman, R. J. Baglan, and B. L. Berman, Phys. Rev. Letters 23, 796 (1969); Phys. Rev. Letters 24, 193E (1970)
[31] B. J. Allen and R. L. Macklin, Phys. Rev. Letters 25, 1675 (1970)
[32] V. Radeka, BNL 16245; also IEE Trans. Nuc. Sci. NS-19, 412 (1972)
[33] R. T. Carpenter, ANL-6589, 1962 (unpublished)
[34] W. R. Kane and M. A. Mariscotti, Nucl. Instr. Meth. 56, 189 (1967)
[35] A. M. Lane, Ann. Phys. 63, 171 (1971)
[36] I. Bergqvist and N. Starfelt, Nucl. Phys. 39, 353 (1962)
[37] S. F. Mughabghab, R. E. Chrien, O. A. Wasson, G. W. Cole, and M. R. Bhat, Phys. Rev. Letters 26, 1118 (1971)
[38] O. A. Wasson, private communication, March 1972
[39] R. C. Block, R. G. Steiglitz, and R. W. Hockenbury, Neutron Cross Sections and Technology, 3rd Conf., CONF-710301, Vol. 2, 889 (1971)
[40] H. E. Jackson and E. N. Strait, Phys. Rev. C4 1314 (1971)
[41] S. F. Mughabghab, R. E. Chrien, and O. A. Wasson, Phys. Rev. Letters 25, 1670 (1970)
[42] M. A. Lone, R. E. Chrien, O. A. Wasson, M. Beer, M. R Bhat, and H. R. Muether, Phys. Rev. 174, 1512 (1968)
[43] O. A. Wasson, R. E. Chrien, G. G. Slaughter, and J. A. Harvey, Phys. Rev. C4, 900 (1971)
[44] P. Axel, Phys. Rev. 126 617 (1962)
[45] N. Rosenzweig, Nucl. Phys. A118, 650 (1968)

[46] G. A. Bartholomew, I. Bergqvist, E. D. Earle, and A. J. Ferguson, Can. J. Phys. 48, 687 (1970)
[47] G. A. Bartholomew, M. R. Gunye, and E. D. Earle, Can. J. Phys. 45, 2063 (1967)
[48] R. Moreh and A. Wolf, Neutron Capture γ-Ray Spectroscopy (Studsvik), IAEA Vienna, 1969, p. 483
[49] R. E. Chrien, K. Rimawi and J. B. Garg, Phys. Rev. C3, 2054 (1971)
[50] E. J. Winhold, E. M. Bowey, D. B. Gayther, and B. H. Patrick, Phys. Letters 32B, 607 (July 1970)
[51] H. E. Jackson, private communication, March 1972